NASA TECHNICAL NOTE

NASA TN D-5487

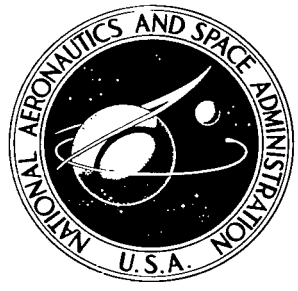

ANALYSIS AND EXPERIMENTS WITH A PULSED NEUTRON SOURCE FOR AN UNREFLECTED SOLUTION REACTOR UP TO $50 SHUTDOWN

by Daniel Fieno, Thomas A. Fox,
Robert A. Mueller, and C. Hubbard Ford

Lewis Research Center
Cleveland, Ohio

NATIONAL AERONAUTICS AND SPACE ADMINISTRATION • WASHINGTON, D. C. • OCTOBER 1969

1. Report No. NASA TN D-5487	2. Government Accession No.	3. Recipient's Catalog No.
4. Title and Subtitle ANALYSIS AND EXPERIMENTS WITH A PULSED NEUTRON SOURCE FOR AN UNREFLECTED SOLUTION REACTOR UP TO $50 SHUTDOWN		5. Report Date October 1969 6. Performing Organization Code
7. Author(s) Daniel Fieno, Thomas A. Fox, Robert A. Mueller, and C. Hubbard Ford		8. Performing Organization Report No. E-5086
9. Performing Organization Name and Address Lewis Research Center National Aeronautics and Space Administration Cleveland, Ohio 44135		10. Work Unit No. 129-02 11. Contract or Grant No.
12. Sponsoring Agency Name and Address National Aeronautics and Space Administration Washington, D. C. 20546		13. Type of Report and Period Covered Technical Note 14. Sponsoring Agency Code
15. Supplementary Notes		

16. Abstract

Pulsed-source experiments have been performed for an unreflected, cylindrical solution reactor for heights varying from delayed critical to highly subcritical systems. The fuel solution consists of enriched (93.2 percent U^{235}) uranyl fluoride salt (UO_2F_2) dissolved in water. For these experiments a hydrogen to U^{235} atom ratio of 975 is used, thus giving highly thermal reactor spectra. Multigroup-transport-theory-calculated values of the fundamental prompt-mode decay constant are compared with experimental values. Also, calculated values for the subcritical reactivity are compared with values obtained from the experiments by using the inhour method, the method of Simmons and King, and the three well-known "area-ratio" methods - those of Garelis and Russell, Sjöstrand, and Gozani.

17. Key Words (Suggested by Author(s)) Solution reactor Pulsed neutron source	18. Distribution Statement Unclassified - unlimited

19. Security Classif. (of this report)	20. Security Classif. (of this page)	21. No. of Pages	22. Price*
Unclassified	Unclassified	59	$3.00

* For sale by the Clearinghouse for Federal Scientific and Technical Information
Springfield, Virginia 22151

CONTENTS

ANALYSIS AND EXPERIMENTS WITH A PULSED NEUTRON SOURCE FOR AN UNREFLECTED SOLUTION REACTOR UP TO $50 SHUTDOWN

by Daniel Fieno, Thomas A. Fox, Robert A. Mueller, and C. Hubbard Ford

Lewis Research Center

SUMMARY

Pulsed-source experiments have been performed using the NASA zero-power solution reactor. This unreflected, homogeneous, thermal reactor provides a simple geometry for assessing the difficulties associated with obtaining shutdown reactivities by using the inhour method, the method of Simmons and King, and the various "area-ratio" techniques. A large range of shutdown reactivity from $0 to $50 was studied.

This study showed that multigroup-transport-theory-calculated values of the fundamental prompt-mode decay constant agree with experimentally determined values to within 5 percent from delayed critical to $5 shutdown; from $5 to $50 the calculated values exceed experiments progressively from 5 to 15 percent. The inhour method and the "area-ratio" techniques of Garelis and Russell and Gozani for obtaining the experimental reactivity gave results that agreed with each other over the range studied. However, the methods of Simmons and King and Sjöstrand considerably underestimated shutdown reactivity over the large range studied. Of all the methods of analyzing the experiments, the inhour method was the most accurate and easy to apply.

INTRODUCTION

There are two basic methods for experimentally determining the reactivity of a subcritical multiplying medium that apply to the pulsed-source technique. One of the methods determines the reactivity from the prompt- and delayed-neutron responses and gives rise to the so-called "area-ratio" techniques. The experiments which use the delayed-neutron response as part of the technique for experimentally determining the subcritical reactivity of a system are also called modified pulsed-source experiments. Three area-ratio techniques for obtaining subcritical reactivities are considered in this study: (1) the area-ratio technique of Sjöstrand (ref. 1), (2) the extrapolated area-ratio tech-

nique of Gozani (ref. 2), and (3) the area-ratio technique of Garelis and Russell (ref. 3).

The other method for experimentally determining the reactivity of a subcritical multiplying medium makes use of the measured fundamental prompt-mode decay constant. Two techniques based on this method are considered in this study. In one technique the subcritical reactivity is obtained by using the measured fundamental prompt-mode decay constant and a calculated parameter. This technique is referred to as the inhour method in this discussion and is described by Preskitt et al. (ref. 4). The other technique, that of Simmons and King (ref. 5), uses only the fundamental prompt-mode decay constants at the subcriticality in question and also at delayed critical.

Modified pulsed-neutron-source techniques for experimentally determining the reactivity of a subcritical multiplying medium have been based on simplified reactor models. The area-ratio method of Sjöstrand is based on monoenergetic diffusion theory applied to an unreflected reactor; the extrapolated area-ratio method of Gozani is based on the assumption that the spatial variation of the delayed modes is the same as that of the fundamental prompt mode; and the technique of Garelis and Russell is also based on monoenergetic diffusion theory applied to an unreflected reactor. However, these experimental techniques are used for complex reactor systems which require correspondingly more complex reactor models. Attempts to improve the theoretical basis of the modified pulsed-neutron-source technique have been made by Corngold (ref. 6), Becker and Quisenberry (ref. 7), Masters and Cady (ref. 8), Wallace et al. (ref. 9), and Preskitt et al. (ref. 4).

The difficulties associated with the various modified pulsed-neutron-source techniques, as well as with the method of Simmons and King, indicate the need for data obtained for systems having a simple geometry. The NASA zero-power solution reactors are convenient for performing pulsed-source experiments and making corresponding calculations for systems ranging from delayed critical to highly subcritical. These reactors use a solution of enriched (93.2 percent uranium-235) uranyl fluoride salt (UO_2F_2) dissolved in water and contained in a cylindrical aluminum vessel. For a given concentration of uranyl fluoride salt in water, criticality is achieved by adjusting the height of the solution. No control rods are associated with these solution reactors. The geometry is thus ideal for performing pulsed-neutron experiments. The reactor used for the pulsed-neutron experiments reported herein is described by Fox et al. (ref. 10). In this report, various important aspects of the experimental procedure, the theoretical basis of the calculations, and the comparison of experimental results with calculations are discussed.

DESCRIPTION OF EXPERIMENTS

Pulsed-neutron-source experiments are straightforward to perform and give a max-

imum of information for the experimental effort involved. The equipment used for this study was high-quality, commercially available equipment with few problems of adaptation. Pulsed-source experiments require a great deal of care in their execution, since a number of variables must be considered. Considerable effort was required to determine the operating variables such as pulse rate, pulse size, source and detector location, analyzer channel width, and operating time. It was also necessary to determine such inherent variables as reactor background, counting system resolution, and water evaporation from the reactor.

In this section, the experimental arrangement, which varies somewhat in detail from the typical pulsed-source setup, is described. The experimental variables are then discussed. Finally, a brief description of the experimental procedures and program is presented.

Experimental Arrangement

Figure 1 is a block diagram of the general experimental arrangement used in this study. A pulsed-neutron source was located external to the solution reactor. Signals from a neutron detector inserted into the solution were sorted as a function of time by using a multichannel analyzer. The pulsed-source unit was used to trigger the analyzer sweep. This arrangement results in one analyzer sweep per pulse of the neutron generator. The number of sweeps, as monitored by a scaler, therefore equaled the number of neutron pulses.

Solution reactor. - Figure 2 shows an elevation view of the reactor tank with the pulsed-neutron source and the neutron detector in typical locations. The reactor is the

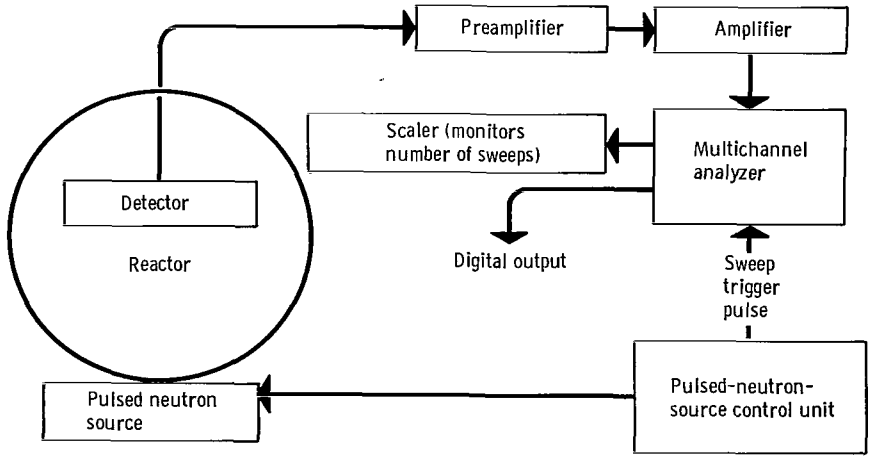

Figure 1. - Diagram of pulsed-neutron-source experiments in NASA solution reactor.

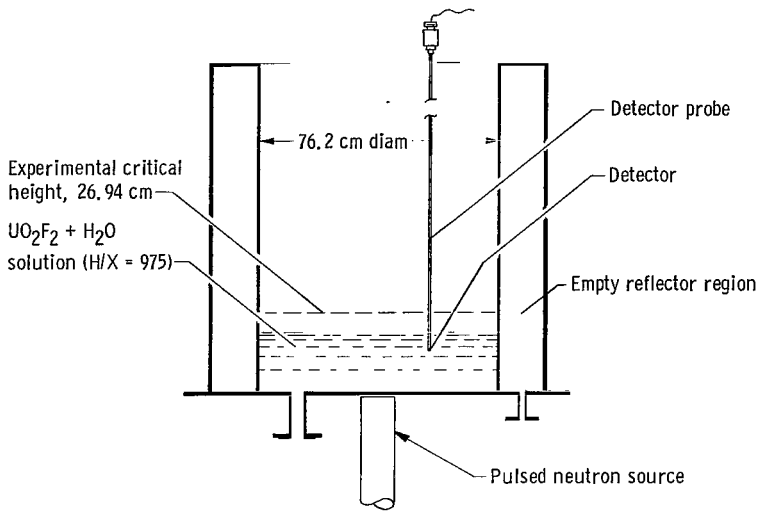

Figure 2. - Typical pulsed-source geometry for unreflected NASA solution reactor. Drawn to scale.

NASA Zero Power Reactor II (ZPR-II). The reactor tank consists of a 76.2-centimeter-diameter by 105-centimeter-tall cylindrical aluminum tank which is open at the top and surrounded by an annular region about 12.5 centimeters thick. This annular region can be used to radially reflect the reactor with water, but no reflector was used in this study. The fuel is a water solution of UO_2F_2 which can be varied over a wide range of concentration but, in this study, was kept fixed near a hydrogen to uranium-235 atom ratio (H/X) of 975. Reactor control is achieved by fuel manipulation. Therefore, a clean system and nearly ideal geometry are readily obtainable. A more complete description of the ZPR-II can be found in reference 10.

Neutron pulse generator. - The neutron pulse generator is a small positive-ion sealed-tube accelerator which produces 14.3-MeV neutrons by means of the $H^3(d,n)He^4$ reaction. The neutron output specifications include a maximum pulse size of the order of 10^7 neutrons per pulse, a pulse width of 3.5 microseconds at half amplitude, and a pulse rate variable from 1 to 11 pulses per second. Pulse size can be varied by changing the acceleration voltage. Pulses are produced by feeding a voltage pulse to the step-up transformer which produces the ion accelerating potential. The active area of the target is about 5 square centimeters, which is small compared to the size of the reactor.

Neutron detectors. - The detector probe which is inserted in the fuel solution is less than 1 centimeter in diameter and has a sensitive volume of 1 cubic centimeter. The small size approximates a point detector and introduces a negligible perturbation. The reactivity worth for this small probe has been measured as less than 7¢ at the center of the core. The small size also makes it possible to find an optimum detector location which enhances the fundamental prompt mode in comparison with the higher-order modes.

The first small probe used in this study was filled with boron trifluoride (BF_3) gas. It was found after a short period of use that tests at or near critical introduced flux fields of sufficient intensity to cause detector performance to deteriorate (the high-voltage plateau would deteriorate). This problem occurred with systems which were shutdown by less than \$3 from delayed critical and got progressively worse as delayed critical was approached.

Substitution of an otherwise identical detector that is filled with helium gas (He^3) was made. The data obtained were consistent and repeatable over the entire range of fuel solution heights including critical and near critical. For cases shutdown by \$3 or more, the data for the BF_3 and He^3 detectors are very similar. Data from both probes are presented in this report.

Multichannel analyzer. - The signals from the detector were fed through a preamplifier and amplifier to a 400-channel analyzer which was operated in the multiscaler mode. In this mode, the channel width is variable. For these experiments, the channel width was varied between 50 and 400 microseconds with a fixed 12.5-microsecond gap between channels to read the data into the memory. System resolution time was measured to be 1.12 microseconds, which made it possible to use a moderately large pulse of neutrons without encountering large deadtime counting losses.

Experimental Variables

The variables associated with this pulsed-neutron-source study are divided into two groups for discussion. Variables which can be readily controlled and changed are covered first. Then variables which are inherent to the physical setup are determined or accounted for.

Experimental variables which can be controlled include neutron pulse size, pulse rate, number of neutron pulses, neutron source location, neutron detector type and detector location, analyzer channel width, and reactor solution height. Among the more important factors which can vary but which are not controlled by the experimenter are various backgrounds, room scatter, water evaporation correction, and neutron source changes with use and age. In addition, such factors as counting system resolution and analyzer channel gap must be determined.

Neutron pulse generator variables. - The neutron generator has been described briefly in the previous section. The energy of the neutrons generated, the width of the pulse, the time delay between the electrical trigger pulse and the neutron pulse, and the physical size (target area) of the source are regarded as fixed. The pulse size, pulse rate, and total number of pulses are considered in this section.

No attempt was made to measure the number of neutrons generated per pulse or to

determine quantitatively how much variation in pulse size occurred. The log N amplifier of the reactor control instrumentation was used to monitor the neutron level throughout the entire experiment. This instrument channel detected and displayed any average change in neutron level over periods of time that are very long compared to the time of a single pulse. The pulse size can be changed by adjusting the accelerator high-voltage pulse size from the control unit. This voltage setting was selected so that the deadtime count loss in the analyzer channel with the most counts was less than 10 percent. In actual practice, only a few percent counting loss occurred in the highest count channels.

The pulse rate is variable over a range from approximately 1 to 11 pulses per second. The effect of pulse rate on experimental results over a range of reactivities was determined. It was found that pulse rate had little effect on results for the range of 3 to 11 pulses per second. From a practical consideration, the highest pulse rate possible should be used to minimize operating time. It was found, however, that 11 pulses per second apparently exceeded the duty cycle of the generator and caused the target to overheat in a short period of time. It was necessary to reduce the pulse rate to 5 to 6 pulses per second in order to give maximum stability to the source output.

The total number of pulses (the operating time) was determined by the requirements for good statistical data. This varies with the configuration involved. For configurations near delayed critical, the prompt-neutron response data determined the amount of pulsing required. For the highly shutdown cases, the delayed-neutron response was the limiting factor. The near critical cases do not present any difficulty since it was easy to get enough counts of both prompt and delayed neutrons in a short operating time. For the highly shutdown cases, it was necessary to pulse for as long as 90 minutes. In general, it was desirable to get about 1000 counts from delayed neutrons (no less than 2 counts in any channel) in order to have sufficiently good statistics for reactivity determination using any of the area-ratio methods. Adequate counts were obtained in the prompt region when this criterion was met in the delayed region for the shutdown cases.

Analyzer channel width. - For the purposes of this study, the multichannel analyzer was always used in a multiscaler mode. The entire 400 channels were employed in all cases. Only the channel width, which was kept as wide as practicable in order to count as many neutrons as possible per pulse, was varied during this study. The channel width was adjusted in general so that at least 25 to 30 channels were available from which to determine the prompt-neutron response.

Source and detector locations. - Preliminary tests were conducted with both the neutron source and a detector external to the reactor core. Although such tests provided useful information regarding the experimental arrangement, no satisfactory pulsed data were obtained. The data were found to be extremely sensitive to the source and detector locations relative to one another. The data were also affected by scattering of neutrons from the walls and structure in the room. It was necessary to insert the detector into

the solution reactor core to alleviate the room scattering problem.

A limited study of the effect of detector position on pulsed-neutron results was carried out. The maximum effect on the decay constant as a result of detector position was of the order of 2 percent total variation. Since the reproducibility of the data is of a similar magnitude, a quantitative result is impractical. There appeared to be a consistent reduction in the decay constant as the detector was moved from the center to the edge of the core in a radial plane, or from midplane to top of the core along an axial line. This effect did not seem to be a function of the magnitude of reactivity shutdown.

The effect of neutron detector location on the reactivity, as determined by the various area-ratio methods, had too many inconsistent data points to ascertain a definite trend. As a consequence, the detector was located at the position which theory indicates should give best results.

With the detector located in the solution, the effect of changing source location appears comparable to changing the pulse size. Different source locations result in a different number of neutrons being injected into the system, but the modal characteristics are essentially a function of system geometry rather than the location of the source.

For these studies the solution had an H/X of 975, and the system had a length to diameter ratio of nearly 1/3. For such conditions the source was most effective when located on the axis of the cylinder near the reactor tank bottom. The detector location used was at a radius of about 16.6 centimeters (0.44 of the radius) and at a height about two-thirds of the core fuel height. The higher modes are minimal with respect to the fundamental mode at this location.

Experimental Program and Procedures

Using the experimental arrangement and experimental variable criteria described in the preceding sections, a series of experiments was made on reactor configurations ranging from the delayed critical condition to highly shutdown systems using a BF_3 detector. These experiments covered several days and were repeated in their entirety several weeks later when a He^3 detector was procured.

When a solution reactor system such as this is operated with its top surface open to the atmosphere, there is a continual evaporation of water from this exposed surface. This evaporation results in a gradual increase in solution concentration which must be continually accounted for and periodically corrected for by the addition of water. This reactor change was determined by running a clean delayed critical case at the beginning of each day's experiments. Corrections to adjust the data to an H/X of 975 were made accordingly. This reference check also assured that the solution concentration was being kept close to an H/X of 975 to keep the corrections as small as possible.

Pulsed experiments at delayed critical. - It was difficult to conduct pulsed-source experiments at delayed critical because of the constantly increasing neutron level with pulsing. It was desirable to achieve criticality at as low a neutron level as practicable for the initial condition. The prompt component was then more readily distinguishable from the steady-state neutron level when the system was pulsed. More important, if the initial neutron level is too high, the operating range of the neutron counting equipment may be exceeded and the deadtime counting losses become excessive before the experiment is completed. As an alternative, the technique suggested in reference 11 was tried. This involves a number of short runs of 30 seconds each in which the neutron level was reduced to some low level after each run. This method did not prove as satisfactory for our study as a single 5-minute run at about 5 to 6 pulses per second where pulse size was kept smaller than for the subcritical runs.

Subcritical pulsed-neutron experiments. - The subcritical configurations were achieved by simply lowering the fuel solution level below the critical height. This resulted in an unperturbed core with a similar clean geometry as in the delayed critical cases. This arrangement permits a study of parameters as a function of fuel height (ΔH below critical) at as many different heights as desired.

When a subcritical configuration is pulsed repetitively, an equilibrium level of delayed neutrons is built up. This neutron level is a function of the pulse rate, the pulse size, and the subcritical state of the system. As soon as the pulsing ceases, this equilibrium level slowly decays to the reactor background level.

In general, more configurations were run at conditions near delayed critical than at the highly shutdown state. Near delayed critical (delayed critical to-\$5), the pulsing time required is short, and the backgrounds can be determined with greater ease and certainty. In order to obtain sufficient data for the highly shutdown cases, the running time per case becomes very long.

When obtaining data to determine reactivity by any of the area-ratio methods, it is essential that both the prompt- and delayed-neutron "areas" be obtained. The fundamental prompt-mode decay constant and prompt area proved easier to measure than the delayed-neutron area. This is due, in part, to the poorer counting statistics for the delayed-neutron response. In addition, the decaying delayed-neutron contribution at the end of pulsing must also be included in the delayed data. The experimental arrangement employed in these tests made such a measurement of the postpulsing response difficult. It was determined by means of a series of experiments that prepulsing the system until its equilibrium delayed-neutron level was obtained (>3 min) provided a method that gave similar results without the need to measure the postpulse decay area. In addition, prepulsing was found desirable, if not necessary, to stabilize the pulse size. When the pulser is started after not pulsing for some time, it frequently takes time for the ion source to come into equilibrium. Until equilibrium occurs, the neutron pulse amplitude

can vary by orders of magnitude. Therefore, all subcritical data reported were obtained by using the prepulse technique. For the critical cases prepulsing was not feasible.

Reactor background. - For each subcritical configuration there is a neutron background that is always present. The nearer to delayed critical, the higher this background level will be. Background was measured at a fixed time after pulsing ceased. It has been determined that most of the cases studied were not particularly sensitive to the reactor background. The reactivity measurements did show some effect from an arbitrary change in background introduced into the data reduction scheme. However, the fundamental prompt-mode decay constant did not change, even when reactor background was arbitrarily increased by a factor of 2 or more.

For critical configurations a neutron level is achieved rather than a background. Because of the nature of critical systems, this can vary widely in magnitude depending on the steady-state power level present. Pulsed critical cases start with as low a level as practicable and end with a higher level, both of which are constant. This area, which corresponds to the delayed-neutron area in a subcritical case, is subtracted from the total data before the fundamental prompt mode decay constant is determined.

ANALYSIS

Analysis of Experimental Data

For a given subcritical solution height, the reactor was pulsed repetitively until adequate counting statistics were obtained. Figure 3 is a schematic representation of the data obtained from an idealized pulsed-source experiment. The background-corrected logarithm of the detector response is plotted as a function of the analyzer channel number. Shown is the equilibrium delayed-neutron contribution persisting after the decay of the prompt-neutron portion of the curve. The slope of the prompt portion of the curve yields the fundamental mode decay constant $(\alpha_0^p)_E$. (All symbols are defined in appendix A.) The areas corresponding to the time integrals of the prompt, as well as the delayed, neutrons are also shown in figure 3.

Appendix B indicates how the experimental data obtained for a subcritical reactor are related to reactivities. The reactivity in dollars for the area-ratio method of Sjöstrand is obtained by taking the ratio of the prompt-neutron area to the delayed-neutron area (refs. 1 and 12); that is,

$$\rho_s^{S0}(\$) = \frac{-\int_0^\infty N_p(\vec{r}, t)dt}{\frac{N_d(\vec{r}, t)}{R}} Z_0^{S0}(\vec{r}) \qquad (B78')$$

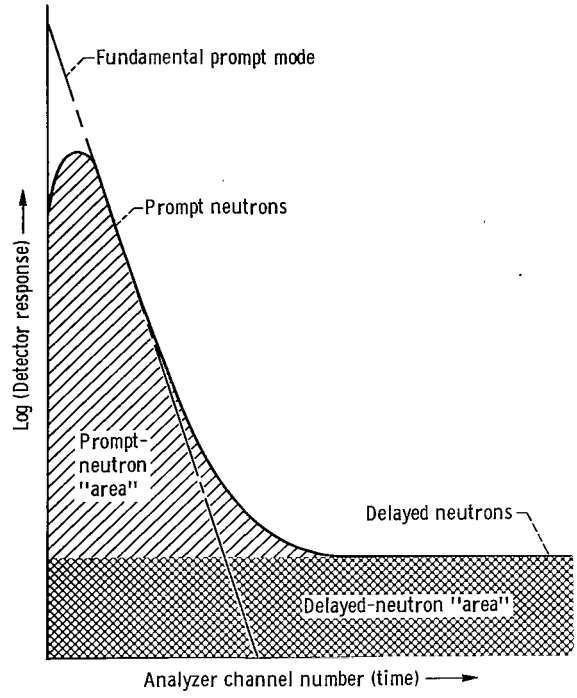

Figure 3. - Ideal detector response to pulsed neutron source.

The quantity $Z_0^{S0}(\vec{r})$ is the spatially dependent kinetic distortion factor which is obtained by calculation using equation (B72'). The reactivity in dollars for the area-ratio method of Gozani is obtained by taking the ratio of the extrapolated fundamental prompt-mode area to the delayed-neutron area; that is,

$$\rho_s^{G0}(\$) = \frac{\dfrac{Q_0 N_0^p(\vec{r})}{(\alpha_0^p)_E}}{\dfrac{N_d(\vec{r},t)}{R}} Z_0^{G0}(\vec{r}) \tag{B76'}$$

The quantity $Z_0^{G0}(\vec{r})$ is the spatially dependent kinetic distortion factor which is obtained by calculation using equation (B53). In the Garelis-Russell method, the prompt-neutron response is weighted by the factor exp(xt), and then integrated over time. The quantity x is adjusted so that this integral equals the prompt- plus delayed-neutron area; that is,

$$\int_0^\infty N_p(\vec{r},t)\exp(xt)dt = \int_0^\infty N_p(\vec{r},t)dt + \frac{N_d(\vec{r},t)}{R} \tag{B54'}$$

Then the reactivity in dollars is given by

$$\rho_s^{GR}(\$) = \left[\frac{\left(\alpha_0^p\right)_E}{x} + 1\right] Z_0^{GR}(\vec{r}) \tag{B77}$$

where the kinetic distortion factor $Z_0^{GR}(\vec{r})$ is equal to $Z_0^{G0}(\vec{r})$. The quantity x in the Garelis-Russell method thus corresponds to the parameter $\bar{\beta}_0/\Lambda_0$, the ratio of the effective delayed-neutron fraction to the generation time for the fundamental prompt mode.

The methods just described for obtaining reactivity are the so-called area-ratio methods. These area-ratio methods are also described as being modified pulsed-source experiments. Reactivity may also be determined from the inhour method by using the measured fundamental prompt-mode decay constant and a calculated value for the parameter $\bar{\beta}_0/\Lambda_0$. This reactivity is given by

$$\rho_s^{IN}(\$) = \frac{\left(\alpha_0^p\right)_E}{\frac{\bar{\beta}_0}{\Lambda_0}} + 1 \tag{B75}$$

Preskitt et al. (ref. 4) discuss the merits of using the inhour method for determining the "experimental" reactivity.

The experimental reactivity may also be determined by the method of Simmons and King (ref. 5). In this method, the fundamental prompt-mode decay constant must be measured at delayed critical and at the subcritical configuration in question. Then the reactivity is given by

$$\rho_s^{SK}(\$) = -\frac{\left(\alpha_0^p\right)_E}{\left(\alpha_0^p\right)_E^{DC}} + 1 \tag{B79}$$

where $\left(\alpha_0^p\right)_E^{DC}$ is the fundamental prompt-mode decay constant at delayed critical.

As indicated, appendix B shows how all of the various equations are derived, while appendix A lists and defines the symbols used. In particular, R is the repetition rate for the pulsed source. Also the kinetic distortion factor for the three area-ratio techniques is a quantitative measure of the spatial and energy differences between the delayed- and prompt-neutron modes.

The reduction of the experimental data into the parameters of interest was carried out by using a digital computer. The computer program GRIPE II developed by Kaufman (ref. 13) was adapted for use on the IBM-7094. This program calculates the fundamental

prompt-mode decay constant, as well as the reactivity, by the area-ratio methods developed by Gozani, Garelis and Russell, and Sjöstrand as discussed previously. An error analysis of each parameter is also carried out by this code, as well as a quality check of the raw data.

After the experimental data have been ordered according to time, they are resolution corrected for counting losses. The reactor background was introduced as a constant for all channels. The experimenter makes a conservative estimate of the number of data channels over which delayed background appears to be constant. The code makes a statistical search to find the best value of the delayed background. The average value of total reactor plus delayed-neutron background is then subtracted from each data point, thus giving the prompt-neutron data. These prompt-neutron data are next examined by the code to find the region of best fit to a negative exponential function. This exponential is assumed to be the fundamental prompt mode. The best fit is determined by a least-squares analysis of the experimental data in which the data are weighted in importance approximately according to the number of counts per data channel. The channels which determine the fundamental prompt-mode region of the decay curve are determined by an iterative calculation which successively rejects channels from each end of the exponential portion of the curve until the best fit is obtained. The initial iteration is chosen to be conservatively large to assure that the best fit is clearly delineated. A chi-square goodness-of-fit test is then applied to assure that the data are described by an exponential.

The reactivity values are determined for all iterations by the code. The reactivity values reported are for the iteration with the best decay curve fit. The error analysis is based on counting statistics only and is not indicative of the absolute accuracy of the experimental data.

Absolute Criticality Calculations

The theoretical basis for the pulsed-source calculation is described fully in appendix B. The S_n method as described in reference 14 was used to obtain solutions to equation (B24) for the fundamental prompt-mode flux and to equation (B13) for the static adjoint flux. One-dimensional slab calculations along the axis of these cylindrical reactor systems were performed by using this method. The aluminum bottom plate was explicitly considered in the transport calculations. The S_4 approximation with elastic neutron scattering treated in the P_1 approximation was found to be adequate in treating the neutron leakage from the ends of these subcritical solution reactors. Radial leakage was calculated from the radial buckling of the system which incorporated transport-theory-calculated extrapolation lengths.

These calculations used eight neutron energy groups, seven fast groups and one ther-

mal group which included an up-scattering transfer component. The fast group cross sections were obtained by using the GAM-II code (ref. 15), and the thermal group cross sections were obtained by using the GATHER-II code (ref. 16). Table I gives the energy boundaries for each neutron energy group. Calculations with this group split have been found to accurately predict the criticality of NASA solution reactors over a large range of hydrogen to U^{235} atom ratios.

Delayed-neutron data used for these calculations were obtained from Keepin (ref. 17, p. 90). Data for U^{235} are listed in table II. For U^{235} the fraction of delayed neutrons produced by fission β was taken to be 0.0065. The average energy of the delayed neutrons varies from about 0.25 to about 1 MeV (ref. 17, p. 95). Thus, all of the spectra for each delayed-neutron group were taken to be in energy group 3.

The solution to equation (B24) gives the fundamental prompt-mode decay constant α_0^p. For a given subcritical system, equation (B24) is solved iteratively until an α_0^p is found such that the reactor multiplication is $1.0/\beta_p$. Then equation (B13) is solved for

TABLE I. - NEUTRON ENERGY GROUP SPLIT

Group	Energy	Lethargy
1	14.92 MeV to 2.231 MeV	-0.4 to 1.5
2	2.231 MeV to 0.821 MeV	1.5 to 2.5
3	0.821 MeV to 0.224 MeV	2.5 to 3.8
4	0.224 MeV to 9.12 keV	3.8 to 7.0
5	9.12 keV to 454 eV	7.0 to 10.0
6	454 eV to 8.32 eV	10.0 to 14.0
7	8.32 eV to 0.414 eV	14.0 to 17.0
8	0.414 eV to 0 eV	17.0 to ∞

TABLE II. - DELAYED-NEUTRON DATA

FOR URANIUM-235

[From ref. 17, p. 90; $\beta = 0.0065$.]

Delayed group	Decay constant, λ, sec^{-1}	Relative abundance, β_i/β	Delayed-neutron fraction, β_i
1	0.0124	0.033	0.000 214 5
2	.0305	.219	.001 423 5
3	.111	.196	.001 274 0
4	.301	.395	.002 567 5
5	1.14	.115	.000 747 5
6	3.01	.042	.000 273 0

the static adjoint flux for the same subcritical system. This immediately gives K_{eff} for this system. The fluxes obtained by solving these two equations are then used to determine the generation time Λ_0 (by using eq. (B15a)) and the effective delayed-neutron fraction $\bar{\beta}_0$ (by using eq. (B19)). These two calculations are sufficient to give the reactivity in dollars from either of the two equations

$$\rho_s^c(\$) = \frac{K_{eff} - 1}{K_{eff}\bar{\beta}_0} \tag{B20a}$$

or

$$\rho_s^c(\$) = \frac{\alpha_0^p}{\frac{\bar{\beta}_0}{\Lambda_0}} + 1 \tag{B20b}$$

These two calculations yield the same result for the static reactivity and can thus be used to check the internal consistency of the computed parameters.

In addition to the calculations described, a solution to equation (B12) for the static flux is needed if kinetic distortion is present in the modified pulsed-source experiments. This spatially dependent factor is given in appendix B for the reactivity methods of Gozani, Garelis and Russell, and Sjöstrand. For these clean, homogeneous, unreflected solution reactors, the assumption is made that kinetic distortion is not present.

RESULTS

Calculated Parameters

Using the methods discussed, calculations and experiments have been performed for a range of fuel solution heights for the NASA Zero Power Solution Reactor (ZPR-II) at a hydrogen to U^{235} atom ratio of 975. The calculated variation with fuel solution height of the reactor parameters required is presented in figure 4. Calculated values of the effective multiplication factor K_{eff} are shown in figure 4(a). The K_{eff} varies from about 0.64 to 1.00 for a fuel solution height varying from about 13 to 26.8 centimeters. The calculations gave a fuel solution height of 26.80 centimeters for the reactor at delayed critical. Figure 4(b) shows the fundamental prompt-mode generation time Λ_0 as a function of fuel solution height. Over the range of fuel solution heights studied, the generation time varies from about 92 to 64 microseconds. Figure 4(c) shows the variation

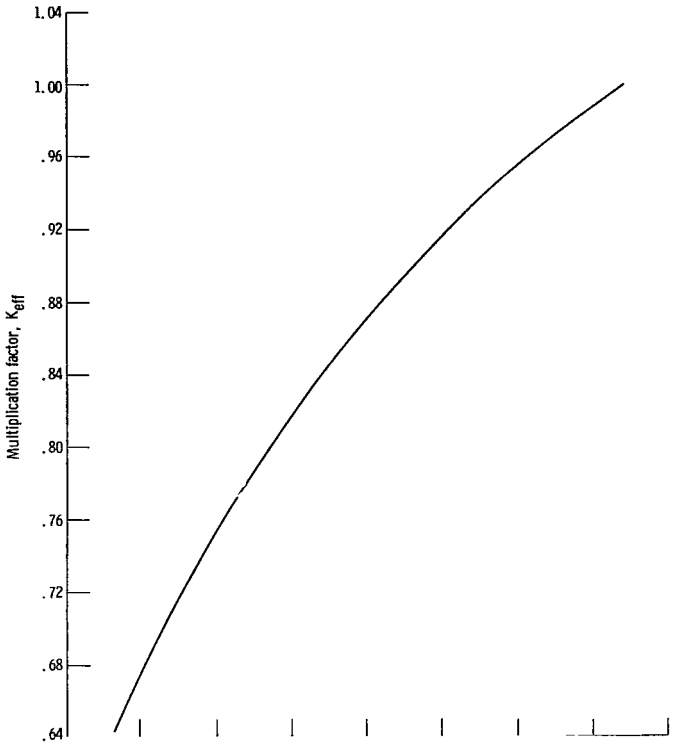

(a) Calculated multiplication factor, K_{eff}.

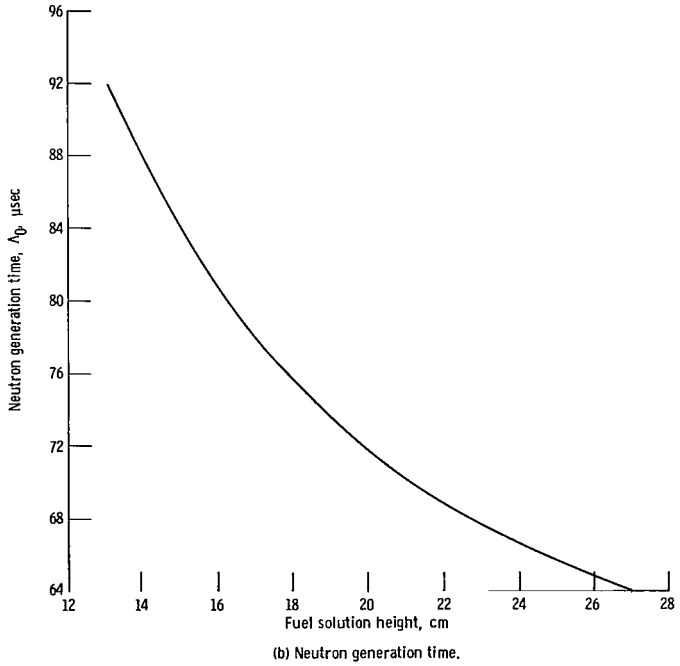

(b) Neutron generation time.

Figure 4. - Variation of reactor parameters with fuel solution height. Unreflected 76.2-centimeter-diameter reactor with fuel solution at hydrogen to uranium-235 atom ratio H/X of 975.

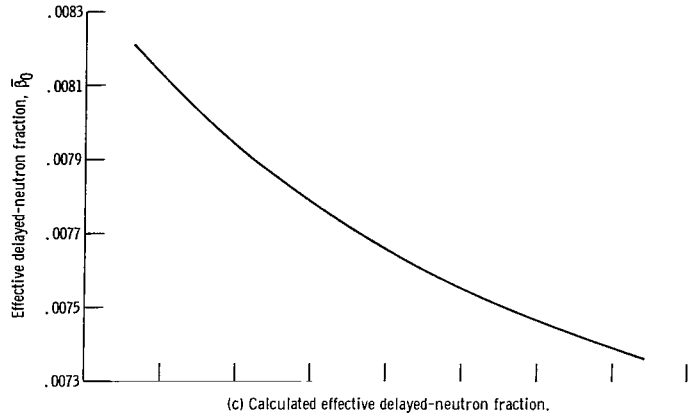

(c) Calculated effective delayed-neutron fraction.

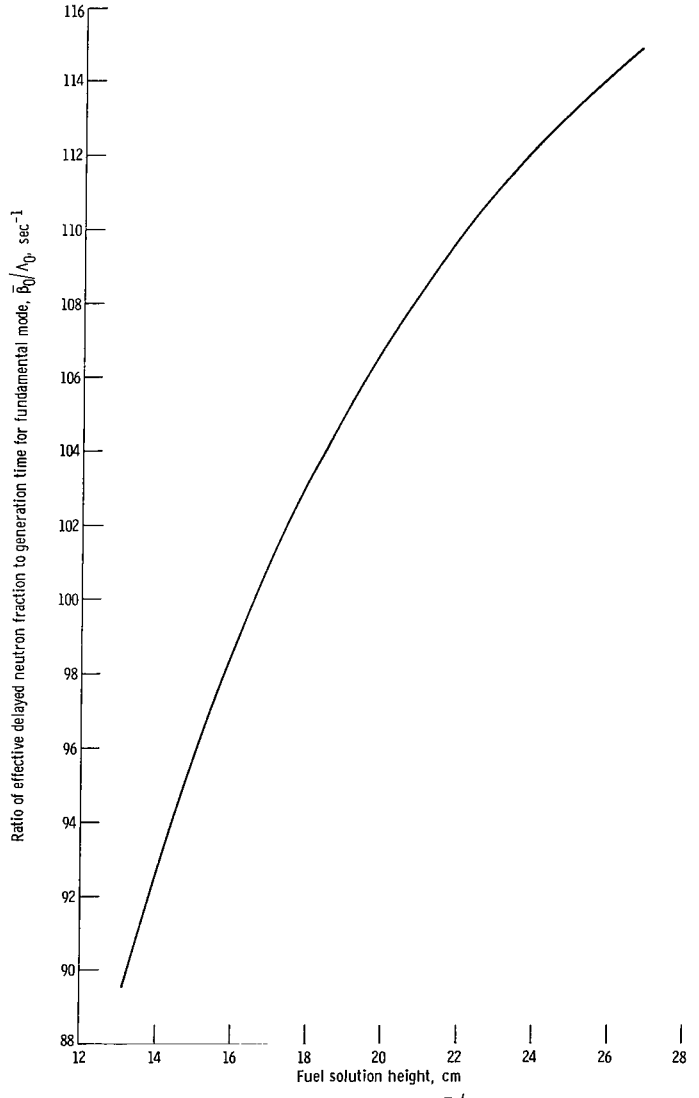

(d) Calculated parameter $\bar{\beta}_0/\Lambda_0$.

Figure 4. - Concluded.

of the fundamental prompt-mode effective delayed-neutron fraction $\overline{\beta}_0$ with solution height. The effective delayed-neutron fraction $\overline{\beta}_0$ varies from about 0.0082 to 0.00736 over the range of fuel solution heights studied. The value of β was taken as 0.0065 for U^{235}. Figure 4(d) shows the variation of the parameter $\overline{\beta}_0/\Lambda_0$ as a function of fuel solution height. This parameter varies from about 89 to 115 per second over the range of fuel solution heights studied.

Comparison of Experiment and Calculation

The experimental results obtained from the pulsed-source study are given as two parameters: (1) the fundamental prompt-mode decay constant and (2) shutdown reactivity values by several techniques. All experimental results are compared with calculated values. The kinetic distortion factor has been taken as 1 for the three area-ratio methods for all subcritical configurations.

Fundamental prompt-mode decay constant. - Figure 5 shows the calculated and experimental values of the fundamental prompt-mode decay constant α_0^p in seconds^{-1} as a function of difference of solution height from delayed critical ΔH in centimeters. The parameter ΔH has been used rather than reactor height for convenience. The experimental critical height at an H/X of 975 has been measured in ZPR-II as 26.94 centimeters as compared to the calculated 26.80 centimeters.

Small variations in reactor temperature and solution concentration from one experimental run to the next are unavoidable with the ZPR-II reactor arrangement. In reducing the raw experimental data, the solution heights were first corrected to room temperature, 20° C, by using the experimentally determined temperature coefficient reported in reference 10. The ΔH values for a given experiment were then normalized to an equivalent ΔH at H/X of 975 by the relation described in appendix B of reference 18. Both corrections are small since the temperature and concentration were not permitted to vary over a large range. These corrections, though small, reduce significantly the scatter present in the uncorrected experimental data.

The experimental data points for α_0^p in figure 5 follow a smooth curve and are in good agreement with calculations. The value of α_0^p at delayed critical is -115 seconds^{-1} for calculation as compared to an average experimental value of -116 seconds^{-1}.

Several data points were repeated a number of times during the course of this study for various reasons. These repeated points give an indication of the reproducibility of the data. An inspection of the data given in table III shows that three data points were repeated exactly. However, a number of points were close enough in ΔH that adjustments could be made to bring the points to the same ΔH for comparison. In the range of ΔH from about 1 to 10 centimeters, the standard deviation in α_0^p is less than 1 percent of

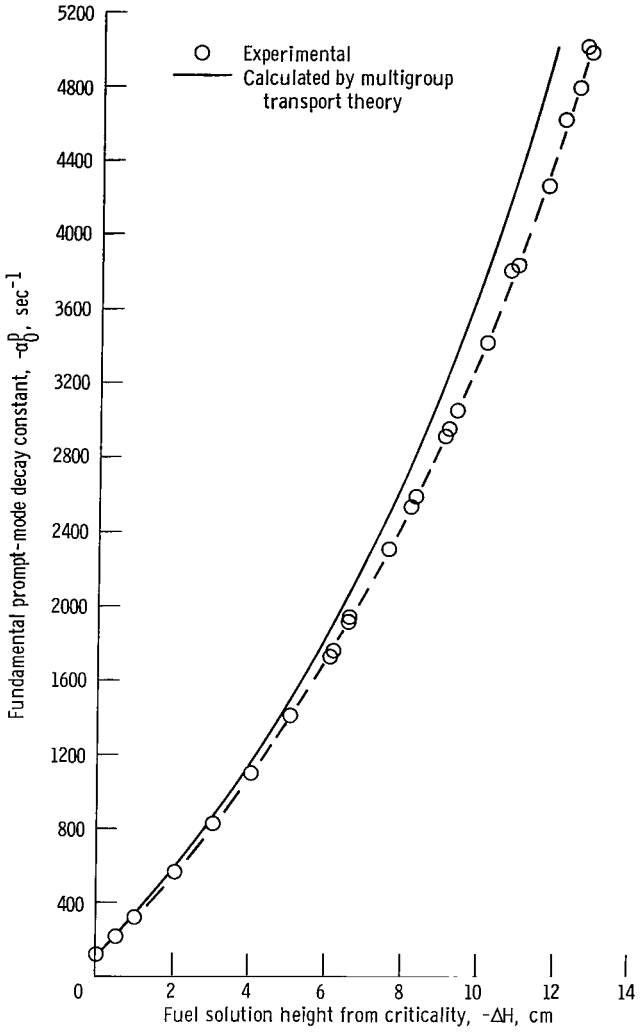

Figure 5. - Fundamental prompt-mode decay constant as function of fuel solution height from criticality at hydrogen to uranium-235 atom ratio H/X of 975.

the value of α_0^p. Beyond 10 centimeters, the standard deviation increases slightly but does not exceed 1.5 percent at the largest ΔH studied. The error limits shown in table III are the standard deviations caused by counting statistics and represent only part of the total problem of reproducibility of the data. For points less than 1-centimeter shutdown, except for the delayed critical case, no deviation determination is possible. In this range, the percentage of uncertainty in ΔH can become a significant factor in the reproducibility of a data point.

A smooth curve drawn through the α_0^p data of figure 5 for ΔH values less than 1 centimeter, but excluding the delayed critical data, was extrapolated to a value of about -115 $seconds^{-1}$ for α_0^p at delayed critical. This is in good agreement with the measured

TABLE III. - EXPERIMENTAL AND CALCULATED VALUES OF

FUNDAMENTAL PROMPT-MODE DECAY CONSTANT

[Unreflected 76.2-cm-diam core with fuel solution of H/X = 975.]

Fuel solution height from criticality,[a] $-\Delta H$, cm	Fundamental prompt-mode decay constant		Fuel solution height from criticality,[a] $-\Delta H$, cm	Fundamental prompt-mode decay constant	
	Experimental,[b] $-(\alpha_0^p)_E$, sec^{-1}	Calculated, $-\alpha_0^p$, sec^{-1}		Experimental,[b] $-(\alpha_0^p)_E$, sec^{-1}	Calculated, $-\alpha_0^p$, sec^{-1}
[c]0	115±0.6	116	6.61	1904±5	2080
[c]0	117±0.6	116	6.65	1937±6	2098
[c].067	126±0.6	130	7.62	2297±7	2500
[c].115	136±0.5	141	8.18	2496±12	2760
[c].251	166±0.5	172	8.22	2524±9	2780
[c].508	218±0.6	230	8.33	2586±8	2830
1.00	330±1	345	9.16	2918±10	3230
[c]1.03	330±1	350	[c]9.17	2938±8	3240
[c]1.04	335±1	355	9.20	2950±11	3250
2.04	568±2	600	9.37	3043±10	3340
[c]2.07	572±1	610	10.18	3417±29	3800
[c]2.11	592±2	617	10.81	3797±15	4180
[c]2.11	591±2	617	10.98	3828±15	4290
3.05	815±2	865	10.98	3820±10	4290
4.06	1096±4	1170	11.77	4252±15	4830
	1092±3	1170	[c]12.20	4607±19	5120
4.06	1091±4	1180	12.22	4604±16	5140
[c]4.08	1404±6	1520	12.58	4782±10	5400
6.10	1732±5	1880	12.74	5008±12	5525
6.18	1749±6	1910	12.88	4977±17	5640
[c]6.60	1914±7	2075			

[a]Experimental delayed critical height, 26.94 cm; calculated delayed critical height, 26.80 cm.

[b]Experimental errors based on counting statistics only.

[c]He^3 detector data, all other data with BF_3 detector.

values of α_0^p at delayed critical which can be found in table III.

The agreement between experimental and calculated α_0^p is best at delayed critical and poorest for the highly shutdown cases. The calculated shutdown values are always larger in absolute magnitude than the experimental values of α_0^p for this fuel concentration. The percentage of difference between calculated and experimental values is less than 10 percent for cases as highly shutdown as \$30, or an α_0^p of -3000. The difference is less than 15 percent out to \$50 shutdown, or an α_0^p of -5000.

The fundamental prompt-mode decay constant is a very sensitive parameter especially near delayed critical. Some idea of the sensitive nature of this parameter can be shown by comparing the difference in calculated and experimental values to the corresponding change in the multiplication constant K_{eff}. For example, near critical a 5 percent change in the decay constant represents about 0.04 percent change in K_{eff}; at about 1 centimeter shutdown a 4 percent change in the decay constant is about 0.1 percent change in K_{eff}; and at about 12 centimeters shutdown a 13 percent change in the decay constant is about a 4.8 percent change in K_{eff}. The numbers given at 1 and 12 centimeters shutdown are the differences between experimental and calculated decay constants.

Determination of shutdown reactivity. - As discussed in the INTRODUCTION, two general methods of determining reactivity values from the experimental data have been used. One method uses the values of α_0^p to determine the reactivity, and the other uses an area-ratio technique of one form or another. Altogether, five different determinations of shutdown reactivity worth are presented for each case measured.

Figure 6(a) is a plot of reactivity as a function of the shutdown fuel height increment ΔH in which calculations with the inhour method and the method of Simmons and King are compared. The solid curve shows the calculated values while a dashed line is used to connect the symbols showing the experimental data. The best agreement with calculations is given by the inhour method $\rho_s^{IN}(\$)$, which uses the experimental α_0^p and calculated values of $\bar{\beta}_0/\Lambda_0$ given in figure 4(d) to determine shutdown reactivity. The Simmons-King method $\rho_s^{SK}(\$)$ gives results in poorer agreement with calculation. This technique assumes that $\bar{\beta}_0/\Lambda_0$ remains constant for all shutdown cases.

Reactivity data as derived from the various area-ratio methods are compared with calculated and inhour method data in figure 6(b). The data given by the Gozani method $\rho_s^{GO}(\$)$ are in the best agreement with the results given by the inhour method and calculations, while the Garelis and Russell $\rho_s^{GR}(\$)$ data approach this agreement. The data from the Sjöstrand method $\rho_s^{SO}(\$)$ are in poor agreement with calculation but are in fair agreement with the Simmons and King data. The reactivity data from all cases considered in this study are given in table IV. More experiments were carried out than are presented in figures 5 and 6. This larger number of experiments was considered necessary in order to establish a degree of confidence in the methods.

In considering the reactivity values derived by using the area-ratio methods, it is

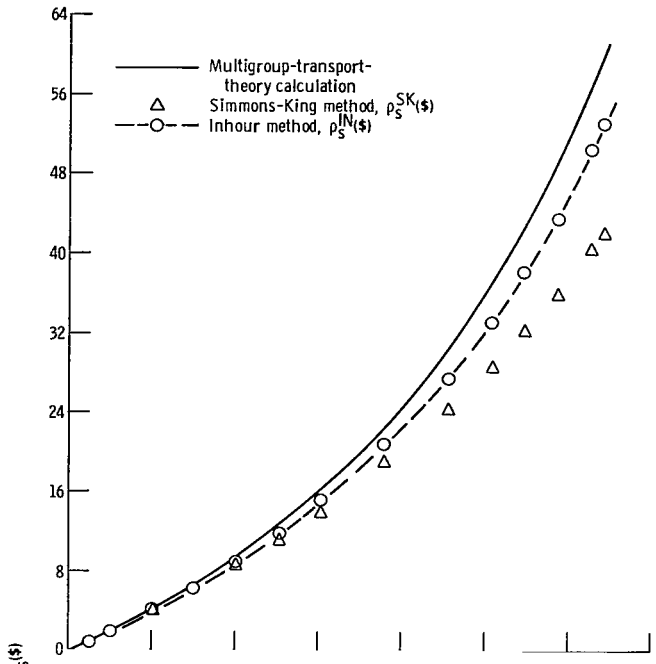

(a) Comparison of calculation with inhour method and method of Simmons and King.

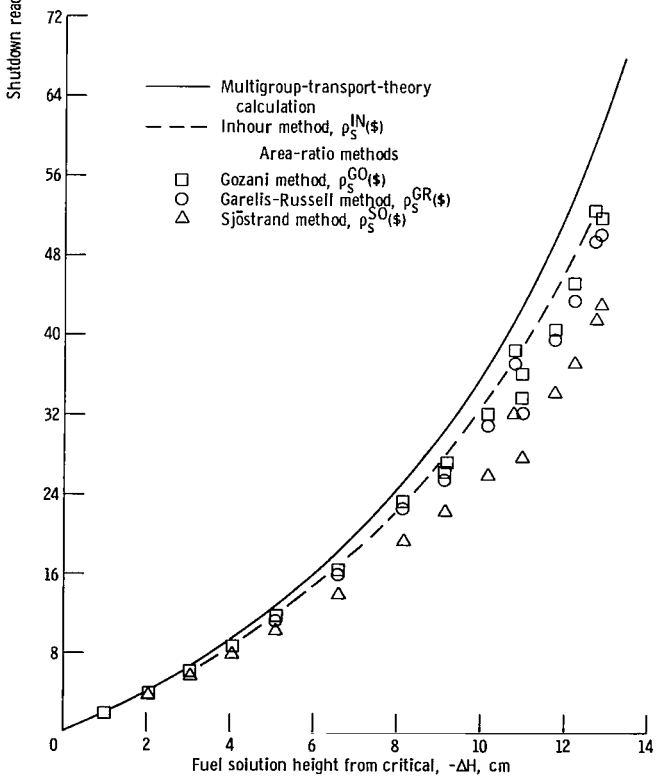

(b) Comparison of calculation with area-ratio methods.

Figure 6. - Shutdown reactivity as function of solution height from criticality at hydrogen to uranium-235 atom ratio H/X of 975.

TABLE IV. - EXPERIMENTAL AND CALCULATED VALUES OF SHUTDOWN REACTIVITY

[Unreflected 76.2-cm-diam core with fuel solution of H/X = 975.]

Fuel solution height from criticality,[a] $-\Delta H$, cm	Shutdown reactivity in dollars					
	Calculated, $-\rho_s^c$	Experimental				
		Inhour method, $-\rho_s^{IN}$	Simmons-King method, $-\rho_s^{SK}$	Area-ratio methods[b]		
				Sjöstrand, $-\rho_s^{S0}$	Garelis-Russell, $-\rho_s^{GR}$	Gozani, $-\rho_s^{G0}$
[c]0.067	0.13	0.10	0.09	0.14±0.001	0.14±0.001	0.14±0.001
[c].115	.23	.18	.17	.21±0.001	.21±0.001	.21±0.001
[c].251	.50	.45	.43	.44±0.001	.46±0.001	.46±0.001
[c].508	1.01	.90	.88	.95±0.004	1.00±0.004	1.00±0.004
1.00	2.03	1.89	1.84	1.81±0.01	1.90±0.01	1.90±0.01
2.04	4.31	4.03	3.90	3.79±0.05	4.03±0.05	4.04±0.05
[c]2.11	4.46	4.24	4.10	3.96±0.05	4.22±0.05	4.23±0.05
2.11	4.46	4.23	4.09	3.83±0.04	4.07±0.04	4.08±0.04
3.05	6.72	6.28	6.03	5.77±0.12	6.20±0.12	6.22±0.12
4.06	9.56	8.89	8.45	7.73±0.14	8.55±0.14	8.64±0.14
4.06	9.56	8.86	8.41	7.97±0.14	8.80±0.14	8.89±0.14
5.11	12.90	11.84	11.10	10.19±0.22	11.49±0.22	11.69±0.22
6.10	16.42	15.05	13.93	13.74±0.37	15.68±0.36	16.02±0.37
6.18	16.71	15.22	14.08	13.66±0.35	15.40±0.35	15.61±0.35
6.61	18.37	16.78	15.41	13.91±0.32	15.98±0.31	16.33±0.32
6.65	18.60	17.09	15.70	13.94±0.35	16.17±0.34	16.70±0.35
7.62	22.72	20.80	18.80	16.96±0.47	19.70±0.46	20.27±0.47
8.18	25.44	22.91	20.52	19.39±0.60	22.75±0.58	23.34±0.60
8.22	25.66	23.20	20.76	19.25±0.57	22.29±0.55	22.79±0.57
8.33	26.20	23.86	21.29	19.96±0.68	23.59±0.65	24.50±0.68
9.16	30.54	27.49	24.16	22.34±0.82	25.48±0.78	26.28±0.82
9.20	30.77	27.84	24.43	23.05±0.87	26.35±0.83	27.20±0.87
9.37	31.76	28.85	25.23	23.14±0.64	27.18±0.62	27.91±0.64
10.18	36.96	33.14	28.46	25.83±0.92	31.01±0.89	32.12±0.92
10.81	41.45	37.56	31.73	32.11±1.5	37.15±1.4	38.75±1.5
10.98	42.73	38.02	32.00	27.83±1.5	32.30±1.4	33.79±1.5
10.98	42.73	37.94	31.93	31.07±0.99	35.26±0.95	36.11±0.99
11.77	49.36	43.34	35.66	34.22±1.5	39.38±1.4	40.62±1.5
12.22	53.44	47.76	38.69	37.25±1.3	43.51±1.2	45.37±1.3
12.58	56.87	50.25	40.22	41.54±1.4	48.34±1.3	50.00±1.4
12.74	58.41	52.85	42.17	41.50±2.2	49.54±2.1	52.64±2.2
12.88	60.07	52.89	41.91	43.09±2.4	50.11±2.3	51.84±2.4

[a]Experimental delayed critical height, 26.94 cm; calculated delayed critical height, 26.80 cm.

[b]Experimental errors based on counting statistics only.

[c]He^3 detector data, all other data with BF_3 detector.

quite apparent that a much greater scatter of data occurs for all three methods than results from the inhour method. This scatter appears to be more a function of the delayed-neutron "area" than the prompt-neutron "area." In particular, the cases with greater shutdown worths suffer from poor statistics. Determination of the channels over which the background is constant is also an important factor. This determination is done by the computer code GRIPE II, as discussed in Analysis of Experimental Data, but judgment on the part of the experimenter is necessary to assure proper use of the code.

CONCLUSIONS

A number of conclusions result from this study of an unreflected homogeneous, thermal reactor from delayed critical to about $50 shutdown:

1. Multigroup-transport-theory-calculated values of the fundamental prompt-mode decay constant agree with experimentally determined values to within 5 percent from delayed critical to $5 shutdown; from $5 to $50 the calculated values exceed experiments progressively from 5 to 15 percent.

2. All methods for determining reactivity experimentally agree to about ±5 percent of the average of all methods for configurations up to $6 shutdown.

3. Experimentally determined reactivities based on the inhour method, which uses the experimental value for the fundamental prompt-mode decay constant and a calculated parameter, had the best agreement with calculations over the range of measurement.

4. The method of Simmons and King gave experimental values for the reactivity which differed considerably from the calculated values over most of the range of solution heights considered. This method fails because the value of the ratio of the effective delayed-neutron fraction to the generation time is not constant with increasing subcriticality.

5. The Garelis-Russell and Gozani area-ratio methods predicted experimental values for the reactivity in agreement with each other and in reasonable agreement with calculations.

6. The area-ratio method of Sjöstrand for determining experimental reactivity was not in agreement with calculated values over the range of the measurements. This method failed because of its more approximate basis as compared to the other two area-ratio methods.

7. All of the area-ratio methods for determining reactivity are sensitive to an accurate experimental determination of the equilibrium delayed-neutron background.

Thus, of the five methods considered for obtaining the shutdown reactivity of the system studied, the inhour method and the Garelis-Russell and Gozani area-ratio methods gave comparable results and agreed reasonably well with calculations. However, all the

area-ratio methods were sensitive to an accurate determination of the delayed-neutron background and exhibited some scatter in the data over the range of measurements considered. In addition, the area-ratio methods are subject to kinetic distortion factors which are quite difficult to compute in practice. The determination of shutdown reactivity by using the inhour method appears to be the most satisfactory over the range of measurements considered. This method does require a calculated parameter, namely the ratio of the effective delayed-neutron fraction to the generation time, which, however, is relatively easy to obtain. The use of the inhour method has another significant advantage over the various area-ratio methods in that the delayed-neutron background is not required, thus considerably simplifying and shortening the run time for an experiment.

Lewis Research Center,
National Aeronautics and Space Administration,
Cleveland, Ohio, August 14, 1969,
129-02.

APPENDIX A

SYMBOLS

$A_j(t)$	j^{th} time-dependent coefficient in expansion of $\phi_p(\vec{r}, E, \vec{\Omega}, t)$ (eq. (B31a))
b_n	coefficient in expansion of time integral of delayed-neutron flux (eq. (B39))
$C_i(\vec{r}, t)$	i^{th} delayed-neutron precursor concentration per unit volume at position $\vec{r}$ at time t, no./(cm^3)(sec)
dE	differential energy element, eV
$d\vec{r}$	differential volume element, cm^3
dt	differential time element, sec
$d\vec{\Omega}$	differential solid angle, sr
E	neutron energy, eV
F_k	integral over reactor volume of product of $P_s^+(\vec{r})$ and $P_k(\vec{r})$ (eq. (B16a))
$F_{k,i}$	integral over reactor volume of product of $P_{s,i}^+(\vec{r})$ and $P_k(\vec{r})$ (eq. (B16b))
F_{nj}	integral over reactor volume of product of $P_n^{s+}(\vec{r})$ and $P_j^p(\vec{r})$ (eq. (B45a))
$F_{nj,i}$	integral over reactor volume of product of $P_{n,i}^{s+}(\vec{r})$ and $P_j^p(\vec{r})$ (eq. (B45b))
F_{00}^s	integral over reactor volume of $P_0^{s+}(\vec{r})$ and $P_0^s(\vec{r})$
$f_i(E)dE$	fraction of neutrons belonging to delayed group i in energy range dE about energy E
$f_k(E)$	kinetic fission spectrum (eq. (B7))
$f_p(E)dE$	fraction of prompt neutrons born in a fission process occurring at any energy and which are found in the energy range dE about energy E
$f_s(E)$	static fission spectrum (eq. (B8))
$G(E' \rightarrow E)dE$	probability that a neutron at energy E' will, after undergoing an (n, 2n) reaction, be in the energy range dE about energy E
$H(E' \rightarrow E)dE$	probability that a neutron at energy E' will, after an inelastic scattering collision, be in the energy range dE about energy E
K_{eff}	neutron multiplication factor
l_k	neutron lifetime for k^{th} prompt mode, sec
l_0	neutron lifetime for fundamental prompt mode, sec

m	number of delayed-neutron emitters for a given fissionable isotope
$N(\alpha_k)$	normalization factor for kinetic fission spectrum (eq. (B9))
$N_d(\vec{r})$	total number of delayed neutrons per unit volume at position $\vec{r}$, no./cm^3 (eq. (B70b))
$N_d(\vec{r}, t)$	total number of delayed neutrons per unit volume at position $\vec{r}$ and at time t, no./(cm^3)(sec) (eq. (B50a))
$N_j^p(\vec{r})$	total number of neutrons of j^{th} prompt mode per unit volume at position $\vec{r}$, no./cm^3 (eq. (B56b))
$N_n^s(\vec{r})$	total number of neutrons of n^{th} static mode per unit volume at position $\vec{r}$, no./cm^3
$N_p(\vec{r})$	total number of prompt neutrons per unit volume at position $\vec{r}$, no./cm^3 (eq. (B70a))
$N_p(\vec{r}, t)$	total number of prompt neutrons per unit volume at position $\vec{r}$, and at time t, no./(cm^3)(sec) (eq. (B56a))
$N_0^p(\vec{r})$	total number of neutrons of fundamental prompt mode per unit volume at position $\vec{r}$, no./cm^3 (eq. (B52a))
$N_0^p(\vec{r}, t)$	total number of fundamental prompt-mode neutrons per unit volume at position $\vec{r}$ and at time t, no./(cm^3)(sec) (eq. (B74))
$n(\vec{r}, E, \vec{\Omega}, t)d\vec{r}\, dE\, d\vec{\Omega}$	probable number of neutrons belonging to space volume element $d\vec{r}$ about position $\vec{r}$, having energies in dE about energy E, and being in the element of solid angle $d\vec{\Omega}$ about $\vec{\Omega}$ at time t
$P(E' \rightarrow E; \mu_L)dE$	probability that a neutron at energy E' will, after an elastic scattering collision, be in the energy range dE about energy E and with the scattering angle being through angle cosine μ_L in the laboratory coordinate system
$P_d(\vec{r})$	number of fission neutrons of all energies produced per unit volume at position $\vec{r}$ for delayed-neutron part of directional neutron flux density, no./(cm^3)(sec) (eq. (B64a))
$P_j^p(\vec{r})$	number of fission neutrons of all energies produced per unit volume at position $\vec{r}$ for j^{th} prompt mode (eq. (B44a))
$P_k(\vec{r})$	number of fission neutrons of all energies produced per unit volume at position $\vec{r}$ for k^{th} prompt mode, no./(cm^3)(sec) (eq. (B16c))
$P_n^s(\vec{r})$	number of fission neutrons of all energies produced per unit volume at position $\vec{r}$ for n^{th} static mode (eq. (B44b))

$P_n^{S+}(\vec{r})$	fission-spectrum-weighted importance function at position $\vec{r}$ for the n^{th} static mode (eq. (B44c))
$P_{n,i}^{S+}(\vec{r})$	i^{th} delayed-neutron-spectrum-weighted importance function at position $\vec{r}$ for n^{th} static mode (eq. (B44d))
$P_p(\vec{r})$	number of fission neutrons of all energies produced per unit volume at position $\vec{r}$ for prompt-neutron part of directional neutron flux density, no./(cm^3)(sec) (eq. (B64b))
$P_s^+(\vec{r})$	static-fission-spectrum-weighted importance at position $\vec{r}$ (eq. (B16d))
$P_{s,i}^+(\vec{r})$	i^{th} delayed-neutron-spectrum-weighted importance function at position $\vec{r}$ (eq. (B16e))
$Q(\vec{r}, E, \vec{\Omega}, t)d\vec{r}\, dE\, d\vec{\Omega}$	number of neutrons produced by a fixed source in space volume element $d\vec{r}$ about position $\vec{r}$, having energies in dE about energy E, and being in the element of solid angle $d\vec{\Omega}$ about $\vec{\Omega}$ at time t
Q_j	coefficient defined by eq. (B38)
$Q_k(\vec{r}, E, \vec{\Omega})d\vec{r}\, dE\, d\vec{\Omega}$	neutrons produced by a fixed source for k^{th} time mode belonging to space volume element $d\vec{r}$ about position $\vec{r}$, and with energies in dE about energy E, and in the element of solid angle $d\vec{\Omega}$ about $\vec{\Omega}$ per sec (eq. (B5b))
Q_0	coefficient for fundamental mode defined by equation (B38)
R	repetition rate for pulsed-neutron source, sec^{-1}
$\vec{R}$	position on surface of reactor system
$\vec{r}$	position vector
s_j	j^{th} coefficient in expansion of $Q(\vec{r}, E, \vec{\Omega}, t)$ (eq. (B31b))
$T_d(t)$	time-dependent function used in separating time-dependence of delayed-neutron directional flux density from its space-energy-angle dependence (eq. (B60b))
$T_p(t)$	time-dependent function used in separating time dependence of prompt-neutron directional flux density from its space-energy-angle dependence (eq. (B60a))
t	time, sec
v(E)	neutron speed corresponding to energy E, cm/sec

x	parameter of Garelis-Russell area-ratio method, defined as a solution of eq. (B54)
$Z^{G0}(\vec{r})$	spatially dependent kinetic distortion factor for extrapolated area-ratio method of Gozani (eq. (B52b))
$Z_0^{G0}(\vec{r})$	spatially dependent kinetic distortion factor for Gozani method for fundamental prompt and delayed modes only (eq. (B53))
$Z^{GR}(\vec{r})$	spatially dependent kinetic distortion factor for Garelis-Russell method (eq. (B58))
$Z_0^{GR}(\vec{r})$	spatially dependent kinetic distortion factor for Garelis-Russell method for fundamental prompt and delayed modes only (eq. (B59))
$Z^{S0}(\vec{r})$	spatially dependent kinetic distortion factor for area-ratio method of Sjöstrand (eq. (B72))
$Z_0^{S0}(\vec{r})$	spatially dependent kinetic distortion factor for Sjöstrand method for fundamental prompt and delayed modes only (eq. (B72'))
α_j^p	decay constant for j^{th} prompt mode, sec^{-1}
α_k	decay constant for k^{th} mode, sec^{-1}
α_k^d	decay constant for k^{th} delayed mode, sec^{-1}
α_0^p	decay constant of fundamental prompt mode, sec^{-1}
$\left(\alpha_0^p\right)_E$	experimentally measured value of fundamental prompt-mode decay constant, sec^{-1}
$\left(\alpha_0^p\right)_E^{DC}$	experimentally measured value of fundamental prompt-mode decay constant for reactor system at delayed critical, sec^{-1}
β	total delayed-neutron fraction per fission for given fissionable isotope, $\beta \equiv \sum_{i=1}^{m} \beta_i$
$\overline{\beta}$	effective delayed-neutron fraction for total prompt flux (eq. (B68))
β_i	fraction of neutrons emitted per fission and belonging to i^{th} delayed group for given fissionable isotope
$\beta_{i,k}$	effective delayed-neutron fraction for i^{th} delayed group and k^{th} prompt mode
$\overline{\beta}_k$	total effective delayed-neutron fraction for k^{th} prompt mode (eq. (B19))
$\overline{\beta}_{nj}$	total effective delayed-neutron fraction for n^{th} delayed mode and j^{th} prompt mode (eq. (B47))

$\beta_{nj,i}$ effective delayed-neutron fraction for i^{th} delayed-neutron group corresponding to n^{th} delayed mode and j^{th} prompt mode (eq. (B46))

β_p fraction of prompt neutrons emitted per fission for given fissionable isotope

$\overline{\beta}_0$ total effective delayed-neutron fraction for fundamental prompt mode

$\overline{\beta}_{00}$ total effective delayed-neutron fraction for fundamental delayed and prompt modes, $\overline{\beta}_{00} = \overline{\beta}_0$

Λ_k generation time for k^{th} prompt mode, sec

Λ_0 generation time for fundamental prompt mode, sec

λ_i decay constant for i^{th} group delayed-neutron precursor, sec^{-1}

μ_L cosine of angle in laboratory coordinate system between initial and final direction of motion of elastically scattered neutron

$\nu(E)$ number of neutrons produced per fission at energy E

ρ_s static reactivity

$\rho_s(\$)$ static reactivity in dollars

$\rho_s^c(\$)$ calculated reactivity in dollars based on either equation (B20a) or (B20b)

$\rho_s^{GR}(\$)$ experimentally determined reactivity in dollars based on Garelis-Russell method (eq. (B77))

$\rho_s^{G0}(\$)$ experimentally determined reactivity in dollars based on Gozani method (eq. (B76))

$\rho_s^{IN}(\$)$ experimentally determined reactivity in dollars based on inhour method (eq. (B75))

ρ_s^n, ρ_s^m reactivity defined for n^{th} and m^{th} static modes

$\rho_s^{SK}(\$)$ experimentally determined reactivity in dollars based on Simmons-King method (eq. (B79))

$\rho_s^{S0}(\$)$ experimentally determined reactivity in dollars based on Sjöstrand method (eq. (B78))

ρ_s^0 reactivity for fundamental delayed mode

$\Sigma_a(E)$ macroscopic neutron absorption cross section at energy E, cm^{-1}

$\Sigma_{es}(E)$ macroscopic neutron elastic scattering cross section at energy E, cm^{-1}

$\Sigma_f(E)$ macroscopic neutron fission cross section at energy E, cm^{-1}

$\Sigma_{in}(E)$ macroscopic neutron inelastic scattering cross section at energy E, cm^{-1}

$\Sigma_{n2n}(E)$	macroscopic neutron (n, 2n) reaction cross section at energy E, cm^{-1}
$\Sigma_t(E)$	macroscopic neutron total cross section at energy E, cm^{-1}, $\Sigma_t(E) = \Sigma_a(E) + \Sigma_{es}(E) + \Sigma_{in}(E) + \Sigma_{n2n}(E)$
$\Sigma_s(E' \rightarrow E; \mu_L)$	generalized scattering kernel (eq. (B10))
τ	width of a source pulse, sec
$\phi(\vec{r}, E, \vec{\Omega}, t)$	directional flux density at point $\vec{r}$ and time t for neutrons of energy E traveling in direction $\vec{\Omega}$, no/(cm^2)(sec)(unit energy)(sr), $\phi(\vec{r}, E, \vec{\Omega}, t) \equiv v(E)n(\vec{r}, E, \vec{\Omega}, t)$
$\phi_d(\vec{r}, E, \vec{\Omega}, t)$	delayed component of $\phi(\vec{r}, E, \vec{\Omega}, t)$, no./$(cm^2)$(sec)(unit energy)(sr)
$\phi_p(\vec{r}, E, \vec{\Omega}, t)$	prompt component of $\phi(\vec{r}, E, \vec{\Omega}, t)$, no./$(cm^2)$(sec)(unit energy)(sr)
$\varphi_d(\vec{r}, E, \vec{\Omega})$	directional delayed-neutron flux density at point $\vec{r}$ for neutrons of energy E traveling in direction $\vec{\Omega}$, no./(cm^2)(sec)(unit energy)(sr) (eq. (B60b))
$\varphi_j^p(\vec{r}, E)$	scalar neutron flux for j^{th} prompt mode at position $\vec{r}$ for neutrons of energy E, no./(cm^2)(sec)(unit energy)
$\varphi_k(\vec{r}, E)$	scalar neutron flux for k^{th} time mode at position $\vec{r}$ for neutrons of energy E, no./(cm^2)(sec)(unit energy)
$\varphi_k(\vec{r}, E, \vec{\Omega})$	directional flux density at point $\vec{r}$ for neutrons of energy E traveling in direction $\vec{\Omega}$ for k^{th} time mode, no./(cm^2)(sec)(unit energy)(sr) (eq. (B5a))
$\varphi_k^d(\vec{r}, E, \vec{\Omega})$	directional flux density at point $\vec{r}$ for neutrons of energy E traveling in direction $\vec{\Omega}$ for k^{th} delayed time mode, no./(cm^2)(sec)(unit energy)(sr)
$\varphi_k^p(\vec{r}, E, \vec{\Omega})$	directional flux density at point $\vec{r}$ for neutrons of energy E traveling in direction $\vec{\Omega}$ for k^{th} prompt time mode, no./(cm^2)(sec)(unit energy)(sr)
$\varphi_k^{p+}(\vec{r}, E, \vec{\Omega})$	adjoint flux corresponding to k^{th} prompt time mode and which gives the importance of neutrons at position $\vec{r}$ which have energy E and are going in direction $\vec{\Omega}$
$\varphi_n^s(\vec{r}, E)$	scalar neutron flux for n^{th} static mode at position $\vec{r}$ for neutrons of energy E, no./(cm^2)(sec)(unit energy)
$\varphi_n^s(\vec{r}, E, \vec{\Omega})$	directional n^{th} mode static flux density at point $\vec{r}$ for neutrons of energy E traveling in direction $\vec{\Omega}$ and corresponding to the reactivity ρ_s^n, no./(cm^2)(sec)(unit energy)(sr) (eq. (B12))

$\varphi_n^{s+}(\vec{r}, E)$ scalar adjoint neutron flux giving importance of neutrons at position $\vec{r}$ and having energy E for the n^{th} static mode

$\varphi_n^{s+}(\vec{r}, E, \vec{\Omega})$ static n^{th} mode adjoint flux defined as a solution to equation (B13) and which gives the importance of neutrons at position $\vec{r}$ which have energy E and are going in direction $\vec{\Omega}$

$\varphi_p(\vec{r}, E, \vec{\Omega})$ directional prompt-neutron flux density at point $\vec{r}$ for neutrons of energy E traveling in direction $\vec{\Omega}$, no./(cm^2)(sec)(unit energy)(sr) (eq. (B60a))

$\varphi_s(\vec{r}, E, \vec{\Omega})$ directional flux density at point $\vec{r}$ for neutrons of energy E traveling in direction $\vec{\Omega}$ corresponding to the reactivity ρ_s, no./(cm^2)(sec)(unit energy)(sr) (eq. (B12))

$\varphi_s^+(\vec{r}, E)$ static adjoint scalar flux giving the importance of neutrons at position $\vec{r}$ and having energy E

$\varphi_s^+(\vec{r}, E, \vec{\Omega})$ static adjoint flux defined as the solution to equation (B13) and which gives the importance of neutrons at position $\vec{r}$ which have energy E and are going in direction $\vec{\Omega}$

$\vec{\Omega}$ unit vector in direction of motion of neutron travel

$\vec{\Omega}^+$ directions which are outwardly directed on surface of reactor

$\vec{\Omega}^-$ directions which are inwardly directed on surface of reactor

\$ unit of reactivity defined such that \$1 represents the amount of reactivity required to change a delayed critical reactor to prompt critical

APPENDIX B

THEORETICAL ANALYSIS

Conventional Static Reactivity

The theory underlying pulsed-neutron-source experiments is based primarily on the analysis given in references 1 to 9 and 12. This appendix is based on the review article of Preskitt et al. (ref. 4) and gives the various equations in conventional rather than operator form. Also the working forms of the various equations are indicated. The equations for the area-ratio method of Sjöstrand are based on reference 12.

To provide a theoretical basis for understanding pulsed-source neutron experiments, consider the time-dependent transport equation with time-independent cross sections and a single fissionable isotope. With these restrictions, the number density of neutrons at position $\vec{r}$ having direction $\vec{\Omega}$ and energy E at time t $n(\vec{r}, E, \vec{\Omega}, t)$ is given by

$$\frac{\partial n(\vec{r}, E, \vec{\Omega}, t)}{\partial t} + \vec{\Omega} \cdot \vec{\nabla} v(E) n(\vec{r}, E, \vec{\Omega}, t) + \Sigma_t(\vec{r}, E) v(E) n(\vec{r}, E, \vec{\Omega}, t)$$

$$= Q(\vec{r}, E, \vec{\Omega}, t) + \iint \Sigma_{es}(\vec{r}, E') v(E') n(\vec{r}, E', \vec{\Omega}', t) P(E' \rightarrow E; \mu_L) dE' \, d\vec{\Omega}'$$

$$+ \frac{1}{4\pi} \iint \Sigma_{in}(\vec{r}, E') v(E') n(\vec{r}, E', \vec{\Omega}', t) H(E' \rightarrow E) dE' \, d\vec{\Omega}'$$

$$+ \frac{1}{4\pi} \iint \Sigma_{n2n}(\vec{r}, E') v(E') n(\vec{r}, E', \vec{\Omega}', t) G(E' \rightarrow E) dE' \, d\vec{\Omega}'$$

$$+ \beta_p \frac{f_p(E)}{4\pi} \iint \nu(\vec{r}, E') \Sigma_f(\vec{r}, E') v(E') n(\vec{r}, E', \vec{\Omega}', t) dE' \, d\vec{\Omega}'$$

$$+ \sum_{i=1}^{m} \lambda_i \beta_i \frac{f_i(E)}{4\pi} \int_{-\infty}^{t} dt' e^{-\lambda_i (t-t')} \iint \nu(\vec{r}, E') \Sigma_f(\vec{r}, E') v(E') n(\vec{r}, E', \vec{\Omega}', t') dE' \, d\vec{\Omega}' \tag{B1}$$

The notation used for equation (B1) is standard, and all symbols are listed in appendix A. The last term on the right side of equation (B1) is given by Gross and Marable (ref. 19).

In equation (B1) the following normalizations are required:

$$\int_E f_p(E)dE = 1.0 \tag{B2a}$$

$$\int_E f_i(E)dE = 1.0 \qquad (i = 1, \ldots, m) \tag{B2b}$$

$$\int_{\vec{\Omega}} d\vec{\Omega} \int_E P(E' \rightarrow E; \mu_L)dE = 1.0 \tag{B2c}$$

$$\int_0^{E'} H(E' \rightarrow E)dE = 1.0 \tag{B2d}$$

$$\int_0^{E'} G(E' \rightarrow E)dE = 2.0 \tag{B2e}$$

The total delayed-neutron fraction β for a given fissionable nuclide is given by

$$\beta = \sum_{i=1}^{m} \beta_i \tag{B3a}$$

and

$$\beta_p + \beta = 1.0 \tag{B3b}$$

Define the directional flux ϕ in equation (B1) in terms of the product vn, that is, let

$$\phi(\vec{r}, E, \vec{\Omega}, t) \equiv v(E)n(\vec{r}, E, \vec{\Omega}, t) \tag{B4}$$

Now solutions to equation (B1) are sought which vary exponentially in time, namely,

$$\phi(\vec{r}, E, \vec{\Omega}, t) = \varphi_k(\vec{r}, E, \vec{\Omega})\exp(\alpha_k t) \tag{B5a}$$

$$Q(\vec{r}, E, \vec{\Omega}, t) = Q_k(\vec{r}, E, \vec{\Omega})\exp(\alpha_k t) \tag{B5b}$$

The expressions given by equations (B4), (B5a), and (B5b) are substituted into equation (B1) and give

$$\vec{\Omega} \cdot \vec{\nabla}\varphi_k(\vec{r}, E, \vec{\Omega}) + \left[\Sigma_t(\vec{r}, E) + \frac{\alpha_k}{v(E)}\right] \varphi_k(\vec{r}, E, \vec{\Omega})$$

$$= Q_k(\vec{r}, E, \vec{\Omega}) + \iint \Sigma_s(\vec{r}, E' \to E; \mu_L)\varphi_k(\vec{r}, E', \vec{\Omega}')dE'\, d\vec{\Omega}'$$

$$+ \frac{f_k(E)}{4\pi} \iint \nu(\vec{r}, E')\Sigma_f(\vec{r}, E')\varphi_k(\vec{r}, E', \vec{\Omega}')dE'\, d\vec{\Omega}' \qquad \text{(B6)}$$

Here $f_k(E)$ defines a kinetic fission spectrum given by

$$f_k(E) = \beta_p f_p(E) + \sum_{i=1}^{m} \frac{\lambda_i \beta_i f_i(E)}{\alpha_k + \lambda_i} = f_s(E) - \sum_{i=1}^{m} \frac{\alpha_k \beta_i f_i(E)}{\alpha_k + \lambda_i} \qquad \text{(B7)}$$

where $f_s(E)$ is the static fission spectrum given by

$$f_s(E) = \beta_p f_p(E) + \sum_{i=1}^{m} \beta_i f_i(E) \qquad \text{(B8)}$$

In the limit as α_k approaches zero, the spectrum $f_k(E)$ approaches the steady-state fission spectrum $f_s(E)$. Since both the prompt and delayed fission spectra are normalized to 1, the kinetic fission spectrum $f_k(E)$ is normalized to

$$\int_E f_k(E)dE = 1 - \sum_{i=1}^{m} \frac{\alpha_k \beta_i}{\alpha_k + \lambda_i} \equiv N(\alpha_k) \qquad \text{(B9)}$$

In equation (B6) the generalized scattering kernel has been defined as

$$\Sigma_s(r, E' \to E; \mu_L) \equiv \Sigma_{es}(r, E')P(E' \to E; \mu_L) + \Sigma_{in}(r, E') \frac{H(E' \to E)}{4\pi} + \Sigma_{n2n}(\vec{r}, E') \frac{G(E' \to E)}{4\pi} \qquad \text{(B10)}$$

Equation (B6) is the expression satisfied by all exponentially varying solutions to equation (B1) and contains no references to the reactivity of the system. Reactivity must then be defined in terms of modal quantities, such as α_k and φ_k, which can be measured. The reactivity used here is the static reactivity ρ_s, which is obtained in conventional reactor calculations. That is, let

$$\rho_s = \frac{K_{eff} - 1}{K_{eff}} \tag{B11}$$

where K_{eff} is the multiplication factor. Thus, the static reactivity ρ_s is obtained as a solution to the equation

$$\vec{\Omega} \cdot \vec{\nabla}\varphi_s(\vec{r}, E, \vec{\Omega}) + \Sigma_t(\vec{r}, E)\varphi_s(\vec{r}, E, \vec{\Omega})$$

$$= \iint \Sigma_s(\vec{r}, E' \rightarrow E; \mu_L)\varphi_s(\vec{r}, E', \vec{\Omega}')dE'\, d\vec{\Omega}'$$

$$+ (1 - \rho_s)\frac{f_s(E)}{4\pi} \iint \nu(\vec{r}, E')\Sigma_f(\vec{r}, E')\varphi_s(\vec{r}, E', \vec{\Omega}')dE'\, d\vec{\Omega}' \tag{B12}$$

Equations (B6) and (B12) are similar in form, with equation (B12) being the equation solved for various reactor analysis problems. However, solutions to equation (B6) may be obtained by using equation (B12) if a term $\alpha_k/v(E)$ is added to $\Sigma_t(\vec{r}, E)$ and if the spectrum $(1 - \rho_s)f_s(E)$ is replaced by the spectrum $f_k(E)$. The source term $Q_k(\vec{r}, E, \vec{\Omega})$ in equation (B6) can be added to equation (B12) if needed.

Inhour Equation

To relate the static reactivity ρ_s to the modal quantities α_k and φ_k write the adjoint of equation (B12), that is,

$$-\vec{\Omega} \cdot \vec{\nabla}\varphi_s^+(\vec{r}, E, \vec{\Omega}) + \Sigma_t(\vec{r}, E)\varphi_s^+(\vec{r}, E, \vec{\Omega})$$

$$= \iint \Sigma_s(\vec{r}, E \rightarrow E'; \mu_L)\varphi_s^+(\vec{r}, E', \vec{\Omega}')dE'\, d\vec{\Omega}'$$

$$+ (1 - \rho_s)\frac{\nu(\vec{r}, E)\Sigma_f(\vec{r}, E)}{4\pi} \iint f_s(E')\varphi_s^+(\vec{r}, E', \vec{\Omega}')dE'\, d\vec{\Omega}' \tag{B13}$$

Now multiply equation (B6) by $\varphi_s^+(\vec{r}, E, \vec{\Omega})$ and integrate over all $d\vec{r}\, dE\, d\vec{\Omega}$; then multiply equation (B13) by $\varphi_k(\vec{r}, E, \vec{\Omega})$ and integrate over all $d\vec{r}\, dE\, d\vec{\Omega}$; now subtract the second equation from the first. The result will be the inhour equation:

$$\rho_s = \alpha_k\left(\Lambda_k + \sum_{i=1}^{m} \frac{\beta_{i,k}}{\alpha_k + \lambda_i}\right) \tag{B14}$$

where the various quantities of equation (B14) are defined as

$$\Lambda_k = \frac{4\pi}{F_k} \iiint \varphi_s^+(\vec{r}, E, \vec{\Omega}) \frac{1}{v(E)} \varphi_k(\vec{r}, E, \vec{\Omega}) d\vec{r}\, dE\, d\vec{\Omega} \tag{B15a}$$

$$\beta_{i,k} = \beta_i \frac{F_{k,i}}{F_k} \tag{B15b}$$

along with

$$F_k = \int P_s^+(\vec{r}) P_k(\vec{r}) d\vec{r} \tag{B16a}$$

$$F_{k,i} = \int P_{s,i}^+(\vec{r}) P_k(\vec{r}) d\vec{r} \tag{B16b}$$

$$P_k(\vec{r}) = \int \nu(\vec{r}, E) \Sigma_f(\vec{r}, E) \varphi_k(\vec{r}, E) dE \tag{B16c}$$

$$P_s^+(\vec{r}) = \int f_s(E) \varphi_s^+(\vec{r}, E) dE \tag{B16d}$$

$$P_{s,i}^+(\vec{r}) = \int f_i(E) \varphi_s^+(\vec{r}, E) dE \tag{B16e}$$

$$\varphi_k(\vec{r}, E) = \int_{\vec{\Omega}} \varphi_k(\vec{r}, E, \vec{\Omega}) d\vec{\Omega} \tag{B16f}$$

$$\varphi_s^+(\vec{r}, E) = \int_{\vec{\Omega}} \varphi_s^+(\vec{r}, E, \vec{\Omega}) d\vec{\Omega} \tag{B16g}$$

To obtain equation (B14), the fixed source term in equation (B6) has been set to zero. The terms involving $\vec{\nabla}\varphi_k(\vec{r}, E, \vec{\Omega})$ and $\vec{\nabla}\varphi_s^+(\vec{r}, E, \vec{\Omega})$ have been eliminated by using Green's theorem along with the boundary conditions

$$\varphi_k(\vec{R}, E, \vec{\Omega}^-) = 0 \tag{B17a}$$

$$\varphi_s^+(R, E, \vec{\Omega}^+) = 0 \tag{B17b}$$

with $\vec{R}$ being on the surface of the reactor system. The direction $\vec{\Omega}^-$ refers to all inwardly directed directions on the reactor surface, while $\vec{\Omega}^+$ refers to all outwardly directed directions.

If α_0^p is the decay constant of the fundamental prompt mode, equation (B14) becomes

$$\rho_s = \alpha_0^p \Lambda_0 + \overline{\beta}_0 \qquad (|\alpha_0^p| \gg \lambda_i,\ i = 1, m) \tag{B18}$$

The quantity $\bar{\beta}_0$ is the effective delayed fraction for the fundamental prompt mode. For the k^{th} prompt mode, the effective delayed-neutron fraction is given by

$$\beta_k = \sum_{i=1}^{m} \beta_{i,k} \tag{B19}$$

Similarly, if Λ_k is defined as the generation time for the k^{th} prompt mode, Λ_0 is the generation time for the fundamental prompt mode.

In terms of dollars, the calculated reactivity (eq. (B11)) is given by

$$\rho_s^c(\$) = \frac{\rho_s}{\bar{\beta}_0} = \frac{K_{eff} - 1}{K_{eff}\bar{\beta}_0} \tag{B20a}$$

The reactivity in dollars as calculated by using equation (B18) is

$$\rho_s^c(\$) = \frac{\rho_s}{\bar{\beta}_0} = \frac{\alpha_0^p}{\frac{\bar{\beta}_0}{\Lambda_0}} + 1 \tag{B20b}$$

If the neutron lifetime, l_k for the k^{th} prompt mode is defined as

$$l_k = K_{eff}\Lambda_k \tag{B21}$$

equations (B14), (B18), and (B20b) may be rewritten in terms of the neutron lifetime, namely,

$$\rho_s = \alpha_k\left(\frac{l_k}{K_{eff}} + \sum_{i=1}^{m} \frac{\beta_{i,k}}{\alpha_k + \lambda_i}\right) \tag{B14'}$$

$$\rho_s = \frac{\alpha_0^p l_0}{K_{eff}} + \bar{\beta}_0 \tag{B18'}$$

$$\rho_s(\$) = \frac{\alpha_0^p}{\frac{K_{eff}\bar{\beta}_0}{l_0}} + 1 \tag{B20b'}$$

Equation (B18) shows that calculated values of Λ_0 and $\bar{\beta}_0$ are required to obtain

the reactivity ρ_s from experimental values of the fundamental prompt-mode decay constant α_0^p. Two static calculations are required so that equation (B18) may be compared to experiment. The first static calculation yields a solution for equation (B12) and gives ρ_s. The second static calculation gives a solution to equation (B6) for α_0^p with the fixed source term set to zero. The spectrum $f_k(E)$ for this calculation, given by equation (B7), goes to

$$f_k(E) = \beta_p f_p(E) \qquad (|\alpha_0^p| \gg \lambda_i,\ i = 1, m) \tag{B22}$$

along with

$$1 - \rho_s = \beta_p \tag{B23}$$

Then, when calculated values of α_0^p and ρ_s are known and $\bar{\beta}_0$ is obtained by some other calculation, equation (B18) can be solved for Λ_0. Finally, when experimental values of α_0^p and the calculated values of Λ_0 and $\bar{\beta}_0$ are used, "experimental" values of the reactivity ρ_s can be obtained by using equation (B18).

Another procedure for obtaining all of the parameters of equation (B18) makes use of the solution to equation (B6) as previously described and the solution to the static adjoint equation given by equation (B13). Then Λ_0 is determined from equation (B15a) and $\bar{\beta}_0$ from equations (B15b) and (B19).

Reactivity from Modal Areas

Expressions can be developed to relate the static reactivity to the modal fluxes and the decay constants. This approach is called a modified pulsed-source technique and the best known methods are those of Gozani (ref. 2), Garelis and Russell (ref. 3), and Sjöstrand (ref. 1).

The distinction between prompt and delayed modes can be seen from equations (B6) and (B7). For prompt modes, $|\alpha_k| \gg \lambda_i$ for all delayed-neutron groups, and the source spectrum is given by equation (B22). The equation for the prompt modes is then

$$\vec{\Omega} \cdot \vec{\nabla}\varphi_k^p(\vec{r}, E, \vec{\Omega}) + \left[\Sigma_t(\vec{r}, E) + \frac{\alpha_k^p}{v(E)}\right]\varphi_k^p(\vec{r}, E, \vec{\Omega})$$
$$= \iint \Sigma_s(\vec{r}, E' \to E; \mu_L)\varphi_k^p(\vec{r}, E', \vec{\Omega}')dE'\, d\vec{\Omega}'$$
$$+ \frac{\beta_p f_p(E)}{4\pi K_{eff}} \iint \nu(\vec{r}, E')\Sigma_f(\vec{r}, E')\varphi_k^p(\vec{r}, E', \vec{\Omega}')dE'\, d\vec{\Omega}' \tag{B24}$$

For delayed modes, the decay constants α_k are known to cluster about the precursor decay constants λ_i, and the term $\alpha_k/v(E)$ in equation (B6) is negligible in comparison to the remaining terms on the left side of the equation. Thus, the delayed modes are given by

$$\vec{\Omega} \cdot \vec{\nabla}\varphi_k^d(\vec{r}, E, \vec{\Omega}) + \Sigma_t(\vec{r}, E)\varphi_k^d(\vec{r}, E, \vec{\Omega})$$

$$= \iint \Sigma_s(\vec{r}, E' \to E; \mu_L)\varphi_k^d(\vec{r}, E', \vec{\Omega}')dE'\, d\vec{\Omega}'$$

$$+ \frac{f_k(E)}{4\pi K_{eff}} \iint \nu(\vec{r}, E')\Sigma_f(\vec{r}, E')\varphi_k^d(\vec{r}, E', \vec{\Omega}')dE'\, d\vec{\Omega}' \qquad \text{(B25)}$$

Comparing equation (B25) with the static equation (eq. (B12)), it can be seen that the solutions for the delayed modes differ from the static flux only in the effect of a different source neutron energy spectrum. The prompt modes differ from these delayed modes by the additional influence of the term $\alpha_k^p/v(E)$ on the neutron spatial and energy distribution. This difference between the prompt and delayed modes is referred to as kinetic distortion.

The small difference between the static and delayed modes caused by the different energy spectrum of source neutrons is ignored. The prompt modes are thus described by equation (B24) and the delayed modes by equation (B12). By writing the adjoint equations corresponding to equations (B12) and (B24), it can be shown that the following orthogonality relations hold:

$$(\alpha_k^p - \alpha_l^p) \iiint d\vec{r}\, dE\, d\vec{\Omega} \left[\varphi_l^{p+}(\vec{r}, E, \vec{\Omega}) \frac{1}{v(E)} \varphi_k^p(\vec{r}, E, \vec{\Omega})\right] = 0 \qquad \text{(B26)}$$

$$\frac{\rho_s^n - \rho_s^m}{4\pi} \int d\vec{r} \iint dE\, d\vec{\Omega}\, \varphi_m^{s+}(\vec{r}, E, \vec{\Omega}) f_s(E)$$

$$\times \iint \nu(\vec{r}, E')\Sigma_f(\vec{r}, E')\varphi_n^s(\vec{r}, E', \vec{\Omega}')dE'\, d\vec{\Omega}' = 0 \qquad \text{(B27)}$$

Equation (B26) states that the prompt adjoint flux is orthogonal to the prompt-neutron density for different prompt modes. Equation (B27) states that the delayed adjoint flux is orthogonal to the delayed fission source for different delayed modes.

A pulsed-neutron transient is now described by assuming that the prompt modes are excited directly by the external source pulse and that the delayed modes are excited by the decay of precursors formed throughout the transient. This is the approach followed in reference 7 and extended by Preskitt et al. in reference 4 to display the role of higher exponential modes, both prompt and delayed, as well as of the kinetic distortion. For

this analysis, it will be convenient to rewrite equation (B1) as (m + 1) time-dependent equations:

$$\frac{1}{v(E)}\frac{\partial\phi(\vec{r},E,\vec{\Omega},t)}{\partial t}+\vec{\Omega}\cdot\vec{\nabla}\phi(\vec{r},E,\vec{\Omega},t)+\Sigma_t(\vec{r},E)\phi(\vec{r},E,\vec{\Omega},t)$$

$$=Q(\vec{r},E,\vec{\Omega},t)+\iint\Sigma_s(\vec{r},E'\rightarrow E;\mu_L)\phi(\vec{r},E',\vec{\Omega}',t)dE'\,d\vec{\Omega}'$$

$$+\frac{\beta_p f_p(E)}{4\pi}\iint\nu(\vec{r},E')\Sigma_f(\vec{r},E')\phi(\vec{r},E',\vec{\Omega}',t)dE'\,d\vec{\Omega}'$$

$$+\frac{\lambda_i C_i(\vec{r},t)f_i(E)}{4\pi} \qquad \text{(B28a)}$$

$$\frac{\partial C_i(\vec{r},t)}{\partial t}=\beta_i\iint\nu(\vec{r},E')\Sigma_f(\vec{r},E')\phi(\vec{r},E',\vec{\Omega}',t)dE'\,d\vec{\Omega}'-\lambda_i C_i(\vec{r},t)$$

$$(i=1,2,\ldots,m) \qquad \text{(B28b)}$$

Equations (B28a) and (B28b) are now written in terms of the prompt component of the angular flux $\phi_p(\vec{r},E,\vec{\Omega},t)$ and the delayed component of the angular flux $\phi_d(\vec{r},E,\vec{\Omega},t)$:

$$\frac{1}{v(E)}\frac{\partial\phi_p(\vec{r},E,\vec{\Omega},t)}{\partial t}+\vec{\Omega}\cdot\vec{\nabla}\phi_p(\vec{r},E,\vec{\Omega},t)+\Sigma_t(\vec{r},E)\phi_p(\vec{r},E,\vec{\Omega},t)$$

$$=Q(\vec{r},E,\vec{\Omega},t)+\iint\Sigma_s(\vec{r},E'\rightarrow E;\mu_L)\phi_p(\vec{r},E',\vec{\Omega}',t)dE'\,d\vec{\Omega}'$$

$$+\frac{\beta_p f_p(E)}{4\pi}\iint\nu(\vec{r},E')\Sigma_f(\vec{r},E')\phi_p(\vec{r},E',\vec{\Omega}',t)dE'\,d\vec{\Omega}' \qquad \text{(B29a)}$$

$$\frac{1}{v(E)}\frac{\partial\phi_d(\vec{r},E,\vec{\Omega},t)}{\partial t}+\vec{\Omega}\cdot\vec{\nabla}\phi_d(\vec{r},E,\vec{\Omega},t)+\Sigma_t(\vec{r},E)\phi_d(\vec{r},E,\vec{\Omega},t)$$

$$=\iint\Sigma_s(\vec{r},E'\rightarrow E;\mu_L)\phi_d(\vec{r},E',\vec{\Omega}',t)dE'\,d\vec{\Omega}'$$

$$+\frac{\beta_p f_p(E)}{4\pi}\iint\nu(\vec{r},E')\Sigma_f(\vec{r},E')\phi_d(\vec{r},E',\vec{\Omega}',t)dE'\,d\vec{\Omega}'+\frac{\lambda_i C_i(\vec{r},t)f_i(E)}{4\pi} \qquad \text{(B29b)}$$

$$\frac{\partial C_i(r,t)}{\partial t} = \beta_i \iint \nu(\vec{r}, E')\Sigma_f(\vec{r}, E')\left[\phi_p(\vec{r}, E', \vec{\Omega}', t) + \phi_d(\vec{r}, E', \vec{\Omega}', t)\right] - \lambda_i C_i(\vec{r}, t) \qquad (i = 1, 2, \ldots, m) \tag{B29c}$$

$$\phi(\vec{r}, E, \vec{\Omega}, t) = \phi_p(\vec{r}, E, \vec{\Omega}, t) + \phi_d(\vec{r}, E, \vec{\Omega}, t) \tag{B29d}$$

Now let a single source pulse occur at time $t = 0$ and integrate equations (B29b) and (B29c) from $t = 0$ to $t = \infty$. Zero initial and final conditions are assumed. If the resulting two equations are now combined by eliminating the term involving the precursor concentration, there results

$$-\left[\vec{\Omega} \cdot \vec{\nabla} + \Sigma_t(\vec{r}, E)\right] \cdot \int_0^\infty \phi_d(\vec{r}, E, \vec{\Omega}, t)dt + \left[\iint dE'\, d\vec{\Omega}'\, \Sigma_s(\vec{r}, E' \to E; \mu_L) + \frac{f_s(E)}{4\pi} \iint dE'\, d\vec{\Omega}'\, \nu(\vec{r}, E')\Sigma_f(\vec{r}, E')\right] \cdot \int_0^\infty \phi_d(\vec{r}, E', \vec{\Omega}', t)dt + \left[\sum_{i=1}^{m} \frac{\beta_i f_i(E)}{4\pi} \iint dE'\, d\vec{\Omega}'\, \nu(\vec{r}, E')\Sigma_f(\vec{r}, E')\right] \cdot \int_0^\infty \phi_p(\vec{r}, E', \vec{\Omega}', t)dt = 0 \tag{B30}$$

This result is obtained for the case of a single pulse; however, the analysis also holds for a repetitively pulsed case (ref. 20). Equation (B30) represents the starting point for obtaining an expression where the modal fluxes are related to the reactivity for the modified pulsed-source technique.

Assume a square source pulse of width τ, expand the prompt flux in terms of the eigenfunctions $\varphi_j^p(\vec{r}, E, \vec{\Omega})$, and also expand the external source in terms of the prompt-neutron densities $v(E)^{-1}\varphi_j^p(\vec{r}, E, \vec{\Omega})$:

$$\phi_p(\vec{r}, E, \vec{\Omega}, t) = \sum_j A_j(t)\varphi_j^p(\vec{r}, E, \vec{\Omega}) \tag{B31a}$$

$$Q(\vec{r}, E, \vec{\Omega}, t<\tau) = \sum_j s_j \frac{1}{v(E)} \varphi_j^p(\vec{r}, E, \vec{\Omega}) \tag{B31b}$$

Substitute equations (B31a) and (B31b) into equation (B29a) and simplify the resulting

equation by using equation (B24). Now multiply the equation by $\varphi_k^{p+}(\vec{r}, E, \vec{\Omega})$ and integrate over all $d\vec{r}\, dE\, d\vec{\Omega}$. Finally, making use of the orthogonality relation given by equation (B26) yields

$$\iiint d\vec{r}\, dE\, d\vec{\Omega} \left[\varphi_j^{p+}(\vec{r}, E, \vec{\Omega}) \frac{1}{v(E)} \varphi_j^{p}(\vec{r}, E, \vec{\Omega})\right]\left\{\frac{dA_j(t)}{dt} - \alpha_j^p A_j(t) - s_j\right\} = 0 \tag{B32}$$

Also, equation (B26) implies that the term in the braces of equation (B32) must be zero, namely,

$$\frac{dA_j(t)}{dt} - \alpha_j^p A_j(t) - s_j = 0 \tag{B33}$$

The solution to the homogeneous form of equation (B33) is

$$A_j(t) = Q_j \exp(\alpha_j^p t) \qquad (t \geq \tau) \tag{B34}$$

where Q_j is, as yet, an undetermined coefficient.

To obtain a solution of equation (B33) for the small time interval from $t = 0$ to $t = \tau$, the following artifice is used. Convert the differential equation to an algebraic equation, that is,

$$\frac{A_j(t)}{t} - \alpha_j^p A_j(t) - s_j = 0 \qquad (t \leq \tau) \tag{B35}$$

which gives

$$A_j(t) = \frac{s_j t}{1 - \alpha_j^p t} \qquad (t \leq \tau) \tag{B36}$$

If the pulse width τ is assumed to be small compared to $1/|\alpha_j^p|$, or equivalently $|\alpha_j^p t| \ll |$, equation (B36) can be written as

$$A_j(t) = s_j t \exp(\alpha_j^p t) \qquad (t \leq \tau) \tag{B37}$$

When $A_j(t)$ from equation (B34) is used, equation (B37) evaluated at $t = \tau$ gives

$$Q_j = \tau s_j \tag{B38}$$

For a square source pulse, s_j is the magnitude independent of t, and Q_j represents the source strength for the j^{th} prompt time mode.

In making the expansions given by equations (B31a) and (B31b), it is assumed that the

prompt modes form a complete set. Thus, the small time interval during which the pulsed-source neutrons are slowed down to fission neutron energies is ignored (ref. 9).

Next expand the delayed flux integral in terms of the static eigenfunctions, that is,

$$\int_0^\infty \phi_d(\vec{r}, E, \vec{\Omega}, t)dt = \sum_n b_n \varphi_n^s(\vec{r}, E, \vec{\Omega}) \tag{B39}$$

Substitute equation (B39) into equation (B30). Multiply the resulting equation by $\varphi_m^{s+}(\vec{r}, E, \vec{\Omega})$ and integrate over all $d\vec{r}\, dE\, d\vec{\Omega}$. Making use of equation (B12) and the orthogonality relation given by equation (B27) results in

$$\iiint d\vec{r}\, dE\, d\vec{\Omega}\ \varphi_n^{s+}(\vec{r}, E, \vec{\Omega}) b_n \cdot \left[-\frac{\rho_s^n f_s(E)}{4\pi} \iint \nu(\vec{r}, E')\Sigma_f(\vec{r}, E')\varphi_n^s(\vec{r}, E', \vec{\Omega}')dE'\, d\vec{\Omega}' \right]$$

$$= \iiint d\vec{r}\, dE\, d\vec{\Omega}\ \varphi_n^{s+}(\vec{r}, E, \vec{\Omega}) \cdot \sum_{i=1}^{m} \frac{\beta_i f_i(E)}{4\pi}$$

$$\cdot \iint dE'\, d\vec{\Omega}'\ \nu(\vec{r}, E')\Sigma_f(\vec{r}, E') \int_0^\infty \phi_p(\vec{r}, E', \vec{\Omega}', t)dt \tag{B40}$$

If equation (B31a) is substituted into the prompt-neutron time integral of equation (B40),

$$\int_0^\infty \phi_p(\vec{r}, E, \vec{\Omega}, t)dt = -\sum_j \frac{\tau s_j}{\alpha_j^p} \varphi_j^p(\vec{r}, E, \vec{\Omega}) \tag{B41}$$

when equations (B34) and (B38) are used. Substitute equation (B41) into equation (B40) and make use of integrals of the type given by equations (B16f) and (B16g), then, solve for b_n:

$$b_n = \frac{\sum_j \frac{Q_j}{\alpha_j^p} \frac{1}{\rho_s^n} \iint d\vec{r}\, dE\ \varphi_n^{s+}(\vec{r}, E) \sum_{i=1}^{m} \frac{\beta_i f_i(E)}{4\pi} \int \nu(\vec{r}, E')\Sigma_f(\vec{r}, E')\varphi_j^p(\vec{r}, E')dE'}{\iint d\vec{r}\, dE\ \varphi_n^{s+}(\vec{r}, E) \frac{f_s(E)}{4\pi} \int \nu(\vec{r}, E')\Sigma_f(\vec{r}, E')\varphi_n^s(\vec{r}, E')dE'} \tag{B42}$$

Now use definitions similar to those given by equations (B16c), (B16d), and (B16e) in equation (B42):

$$b_n = \frac{\sum_j \frac{Q_j}{\alpha_j^p \rho_s^n} \sum_{i=1}^{m} \int d\vec{r}\, P_{n,i}^{s+}(\vec{r}) P_j^p(\vec{r})}{\int d\vec{r}\, P_n^{s+}(\vec{r}) P_n^s(\vec{r})} \tag{B43}$$

Explicitly written, these definitions are

$$P_j^p(\vec{r}) = \int \nu(\vec{r}, E)\Sigma_f(\vec{r}, E)\varphi_j^p(\vec{r}, E)dE \tag{B44a}$$

$$P_n^s(\vec{r}) = \int \nu(\vec{r}, E)\Sigma_f(\vec{r}, E)\varphi_n^s(\vec{r}, E)dE \tag{B44b}$$

$$P_n^{s+}(\vec{r}) = \int f_s(E)\varphi_n^{s+}(\vec{r}, E)dE \tag{B44c}$$

$$P_{n,i}^{s+}(\vec{r}) = \int f_i(E)\varphi_n^{s+}(\vec{r}, E)dE \tag{B44d}$$

Define modal quantities similar to those given by equations (B16a) and (B16b):

$$F_{nj} = \int P_n^{s+}(\vec{r}) P_j^p(\vec{r}) d\vec{r} \tag{B45a}$$

$$F_{nj,i} = \int P_{n,i}^{s+}(\vec{r}) P_j^p(\vec{r}) d\vec{r} \tag{B45b}$$

Now define the effective modally dependent delayed-neutron fraction as

$$\beta_{nj,i} = \frac{\beta_i F_{nj,i}}{F_{nj}} \tag{B46}$$

along with

$$\bar{\beta}_{nj} = \sum_{i=1}^{m} \beta_{nj,i} = \sum_{i=1}^{m} \frac{\beta_i F_{nj,i}}{F_{nj}} \tag{B47}$$

Substitute equation (B45b) in equation (B43) and then use equations (B47) and (B45a) to obtain the following result for b_n:

$$b_n = \sum_j \left(\frac{Q_j}{\alpha_j^p}\right)\left(\frac{\bar{\beta}_{nj}}{\rho_s^n}\right) \frac{\int P_n^{s+}(\vec{r}) P_j^p(\vec{r}) d\vec{r}}{\int P_n^{s+}(\vec{r}) P_n^s(\vec{r}) d\vec{r}} \tag{B48}$$

With this solution for the delayed modes, measurable quantities may be expressed in a a form which yields reactivity. This is done by substituting for b_n in equation (B39) its value from equation (B48). Then this resulting expression is multiplied by $v(E)^{-1}$ and integrated over all energies and all values of $\vec{\Omega}$. The resulting expression is given by

$$\int_0^\infty N_d(\vec{r}, t)dt = \sum_n \sum_j \left(\frac{Q_j}{\alpha_j^p}\right)\left(\frac{\bar{\beta}_{nj}}{\rho_s^n}\right) \frac{\int P_n^{s+}(\vec{r}) P_j^p(\vec{r}) d\vec{r}}{\int P_n^{s+}(\vec{r}) P_n^s(\vec{r}) d\vec{r}} N_n^s(\vec{r}) \tag{B49}$$

where

$$N_d(\vec{r}, t) = \int dE \frac{1}{v(E)} \int d\vec{\Omega}\ \phi_d(\vec{r}, E, \vec{\Omega}, t) \tag{B50a}$$

$$N_n^s(\vec{r}) = \int dE \frac{1}{v(E)} \int d\vec{\Omega}\ \varphi_n^s(\vec{r}, E, \vec{\Omega}) \tag{B50b}$$

Rearranging equation (B49) to extract the reactivity in dollars for the fundamental mode yields

$$\rho_s(\$) = \frac{\rho_s^0}{\bar{\beta}_{00}}$$

$$= \frac{\dfrac{Q_0 N_0^p(\vec{r})}{\alpha_0^p}}{\displaystyle\int_0^\infty N_d(\vec{r}, t)dt} Z^{G0}(\vec{r}) \tag{B51}$$

where

$$N_0^p(\vec{r}) = \int dE \frac{1}{v(E)} \int d\vec{\Omega}\ \varphi_0^p(\vec{r}, E, \vec{\Omega}) \tag{B52a}$$

$$Z^{G0}(\vec{r}) = \sum_{n} \sum_{j} \left(\frac{Q_j}{Q_0}\right)\left(\frac{\alpha_0^p}{\alpha_j^p}\right)\left(\frac{\frac{\rho_s^0}{\bar{\beta}_{00}}}{\frac{\rho_s^n}{\bar{\beta}_{nj}}}\right) \cdot \frac{\int P_n^{s+}(\vec{r})P_j^p(\vec{r})d\vec{r}}{\int P_n^{s+}(\vec{r})P_n^s(\vec{r})d\vec{r}} \cdot \frac{N_n^s(\vec{r})}{N_0^p(\vec{r})} \qquad \text{(B52b)}$$

Equation (B51) is the fundamental relation for the interpretation of the modified pulsed-source method known as the Gozani or "extrapolated area-ratio" method (ref. 2). The quantity $Z^{G0}(\vec{r})$ is space dependent and is called the kinetic distortion factor.

Preskitt et al. (ref. 4) make the following observations concerning the space-dependent correction factor $Z^{G0}(\vec{r})$:

(1) If kinetic distortion is present, all orders of delayed harmonics appear, even though only the fundamental prompt mode is excited by the pulsed source.

(2) If no kinetic distortion is present, a given delayed mode appears only if the corresponding prompt mode is excited by the pulsed source.

(3) The influence of the delayed harmonics is suppressed by factors Q_j/Q_0, α_0^p/α_j^p, and ρ_0/ρ_n, and the space dependence of the correction factor tends strongly to the ratio of the fundamental delayed and prompt modes.

The last consideration discussed concerning the kinetic distortion factor suggests evaluation of $Z^{G0}(\vec{r})$ for the fundamental delayed $n = 0$ and prompt $j = 0$ modes only. This gives $Z^{G0}(\vec{r})$ as

$$Z_0^{G0}(\vec{r}) = \frac{N_0^s(\vec{r})}{N_0^p(\vec{r})} \cdot \frac{\int P_0^{s+}(\vec{r})P_0^p(\vec{r})d\vec{r}}{\int P_0^{s+}(\vec{r})P_0^s(\vec{r})d\vec{r}} \qquad \text{(B53)}$$

which can be calculated relatively easily.

The space dependence of other modified pulsed-source methods can also be expressed in terms of the prompt amplitudes of equation (B34) and the delayed-neutron integral given by equation (B49). The β/Λ method of Garelis and Russell (ref. 3) is obtained by assuming the following relation between $N_p(\vec{r},t)$ and $N_d(\vec{r},t)$ for some constant x:

$$\int_0^\infty N_p(r,t)[\exp(xt) - 1]dt = \int_0^\infty N_d(\vec{r},t)dt \qquad \text{(B54)}$$

The equations (B31a) and (B34) are used to obtain

$$N_p(\vec{r},t) = \sum_j Q_j \exp(\alpha_j^p t)N_j^p(\vec{r}) \qquad \text{(B55)}$$

where

$$N_p(\vec{r},t) = \int dE \frac{1}{v(E)} \int d\vec{\Omega}\ \phi_p(\vec{r},E,\vec{\Omega},t) \tag{B56a}$$

$$N_j^p(\vec{r}) = \int dE \frac{1}{v(E)} \int d\vec{\Omega}\ \varphi_j^p(\vec{r},E,\vec{\Omega}) \tag{B56b}$$

Now substitute equations (B49) and (B55) into equation (B54) Perform the integration over time, and rearrange the equation in a form such that the reactivity may be extracted. Then, solving for the reactivity in dollars yields

$$\rho_s(\$) = \frac{\rho_s^0}{\bar{\beta}_{00}} = \left(1 + \frac{\alpha_0^p}{x}\right) Z^{GR}(\vec{r}) \tag{B57}$$

where

$$Z^{GR}(\vec{r}) = \frac{\displaystyle\sum_n \sum_j \left(\frac{Q_j}{\alpha_j^p}\right)\left(\frac{\frac{\rho_s^0}{\bar{\beta}_{00}}}{\frac{\rho_s^n}{\bar{\beta}_{nj}}}\right) \cdot \frac{\int P_n^{s+}(\vec{r})P_j^p(\vec{r})d\vec{r}}{\int P_n^{s+}(\vec{r})P_n^s(\vec{r})d\vec{r}} \cdot N_n^s(\vec{r})}{\displaystyle\sum_j \left(\frac{Q_j}{\alpha_j^p}\right) \cdot \left(\frac{1+\frac{\alpha_0^p}{x}}{1+\frac{\alpha_j^p}{x}}\right) \cdot N_j^p(\vec{r})} \tag{B58}$$

Similar remarks apply to equation (B57) concerning the spatially dependent kinetic distortion factor $Z^{GR}(\vec{r})$ as apply to equation (B51) and $Z^{G0}(\vec{r})$. Evaluating the kinetic distortion factor $Z^{GR}(\vec{r})$ for the fundamental delayed $n = 0$ and prompt $j = 0$ modes only gives

$$Z_0^{GR}(\vec{r}) = \frac{N_0^s(\vec{r})}{N_0^p(\vec{r})} \cdot \frac{\int P_0^{s+}(\vec{r})P_0^p(\vec{r})d\vec{r}}{\int P_0^{s+}(\vec{r})P_0^s(\vec{r})d\vec{r}} \tag{B59}$$

Thus, we have established that $Z_0^{GR}(\vec{r}) \equiv Z_0^{G0}(\vec{r})$. In other words, the kinetic distortion correction factor based on the fundamental delayed and prompt modes only is the same

for the Gozani and Garelis-Russell modified pulsed-source techniques.

The area-ratio method of Sjöstrand can be derived by using equations (B29b) and (B29c). As before, let a single source pulse occur at time $t = 0$ and integrate equations (B29b) and (B29c) from $t = 0$ to $t = \infty$. Zero initial and final conditions are assumed. Combine the resulting two equations by eliminating the term involving the precursor concentration to obtain equation (B30). Now assume that the delayed- and prompt-neutron fluxes are separable into a time-dependent part and a position-energy-angle part. That is, let

$$\phi_p(\vec{r}, E, \vec{\Omega}, t) = \varphi_p(\vec{r}, E, \vec{\Omega}) T_p(t) \tag{B60a}$$

$$\phi_d(\vec{r}, E, \vec{\Omega}, t) = \varphi_d(\vec{r}, E, \vec{\Omega}) T_d(t) \tag{B60b}$$

Substitute equations (B60a) and (B60b) in (B30). This gives

$$\frac{\int_0^\infty T_p(t)dt}{\int_0^\infty T_d(t)dt} = \frac{\left[\vec{\Omega}\cdot\vec{\nabla}\varphi_d(\vec{r}, E, \vec{\Omega}) + \Sigma_t(\vec{r}, E)\varphi_d(\vec{r}, E, \vec{\Omega}) - \iint \Sigma_s(\vec{r}, E' \to E; \mu_L)\varphi_d(\vec{r}, E', \vec{\Omega}')dE'\, d\vec{\Omega}' - \frac{f_s(E)}{4\pi}\iint \nu(\vec{r}, E')\Sigma_f(\vec{r}, E')\varphi_d(\vec{r}, E', \vec{\Omega}')dE'\, d\vec{\Omega}'\right]}{\sum_{i=1}^{m} \frac{\beta_i f_i(E)}{4\pi} \iint \nu(\vec{r}, E')\Sigma_f(\vec{r}, E')\varphi_p(\vec{r}, E', \vec{\Omega}')dE'\, d\vec{\Omega}'} \tag{B61}$$

Before it was assumed that the delayed modes satisfy equation (B12), and now it is assumed that $\varphi_d(\vec{r}, E, \vec{\Omega})$ will also satisfy equation (B12). This equation is now substituted into equation (B61) to give

$$\frac{\int_0^\infty T_p(t)dt}{\int_0^\infty T_d(t)dt} = \frac{-\frac{\rho_s f_s(E)}{4\pi} \iint \nu(\vec{r}, E')\Sigma_f(\vec{r}, E')\varphi_d(\vec{r}, E', \vec{\Omega}')dE'\, d\vec{\Omega}'}{\sum_{i=1}^{m} \frac{\beta_i f_i(E)}{4\pi} \iint \nu(\vec{r}, E')\Sigma_f(\vec{r}, E')\varphi_p(\vec{r}, E', \vec{\Omega}')dE'\, d\vec{\Omega}'} \tag{B62}$$

Multiply the numerator and denominator of equation (B62) by the adjoint flux $\varphi_s^+(\vec{r}, E, \vec{\Omega})$ which is a solution of equation (B13), and integrate over all energies E and over all directions $\vec{\Omega}$. The result is

$$\frac{\int_0^\infty T_p(t)dt}{\int_0^\infty T_d(t)dt} =$$

$$\frac{-\frac{\rho_s}{4\pi}\iint f_s(E)\varphi_s^+(\vec{r}, E, \vec{\Omega})dE\, d\vec{\Omega} \iint \nu(\vec{r}, E')\Sigma_f(\vec{r}, E')\varphi_d(\vec{r}, E', \vec{\Omega}')dE'\, d\vec{\Omega}'}{\sum_{i=1}^{m}\iint \frac{\beta_i f_i(E)}{4\pi}\varphi_s^+(\vec{r}, E, \vec{\Omega})dE\, d\vec{\Omega} \iint \nu(\vec{r}, E')\Sigma_f(\vec{r}, E')\varphi_p(\vec{r}, E', \vec{\Omega}')dE'\, d\vec{\Omega}'} \tag{B63}$$

Analogous to equation (B16c) define

$$P_d(\vec{r}) = \iint \nu(\vec{r}, E')\Sigma_f(\vec{r}, E')\varphi_d(\vec{r}, E', \vec{\Omega}')dE'\, d\vec{\Omega}' \tag{B64a}$$

$$P_p(\vec{r}) = \iint \nu(\vec{r}, E')\Sigma_f(\vec{r}, E')\varphi_p(\vec{r}, E', \vec{\Omega}')dE'\, d\vec{\Omega}' \tag{B64b}$$

Now integrate equation (B63) over $\vec{\Omega}$. Then, use equations (B16d), (B16e), (B64a), and (B64b) to obtain

$$\frac{\int_0^\infty T_p(t)dt}{\int_0^\infty T_d(t)dt} = \frac{-\rho_s P_s^+(\vec{r})P_d(\vec{r})}{\sum_{i=1}^{m}\beta_i P_{s,i}^+(\vec{r})P_p(\vec{r})} \tag{B65}$$

Integrate the right side of equation (B65) over the volume of the system:

$$\frac{\int_0^\infty T_p(t)dt}{\int_0^\infty T_d(t)dt} = \frac{-\rho_s \int P_s^+(\vec{r})P_d(\vec{r})d\vec{r}}{\sum_{i=1}^{m}\beta_i \int P_{s,i}^+(\vec{r})P_p(\vec{r})d\vec{r}} \tag{B66}$$

Then, using equations (B15b) and (B19) and assuming that $P_d(\vec{r}) \approx P_p(\vec{r})$ yields

$$\rho_s(\$) = \frac{\rho_s}{\bar{\beta}} = \frac{-\int_0^\infty T_p(t)dt}{\int_0^\infty T_d(t)dt} \cdot \frac{\int P_s^+(\vec{r})P_p(\vec{r})d\vec{r}}{\int P_s^+(\vec{r})P_d(\vec{r})d\vec{r}} = -\frac{\int_0^\infty T_p(t)dt}{\int_0^\infty T_d(t)dt} \tag{B67}$$

where $\overline{\beta}$ is defined as

$$\overline{\beta} = \frac{\sum_{i=1}^{n} \beta_i \iint P_{s,i}^{+}(\vec{r}) P_p(\vec{r}) d\vec{r}}{\iint P_s^{+}(\vec{r}) P_p(\vec{r}) d\vec{r}} \tag{B68}$$

Multiply equations (B60a) and (B60b) by $1/v(E)$ and then integrate over all energies E and all directions of motion $\vec{\Omega}$. The result is

$$N_p(\vec{r}, t) = N_p(\vec{r}) T_p(t) \tag{B69a}$$

$$N_d(\vec{r}, t) = N_d(\vec{r}) T_d(t) \tag{B69b}$$

where $N_p(\vec{r})$ and $N_d(\vec{r})$ are defined by the equations

$$N_p(\vec{r}) = \int dE \frac{1}{v(E)} \int d\vec{\Omega}\, \varphi_p(\vec{r}, E, \vec{\Omega}) \tag{B70a}$$

$$N_d(\vec{r}) = \int dE \frac{1}{v(E)} \int d\vec{\Omega}\, \varphi_d(\vec{r}, E, \vec{\Omega}) \tag{B70b}$$

Substitute equations (B69a) and (B69b) into equation (B67). The result is the area-ratio method of Sjöstrand, that is,

$$\rho_s(\$) = -\frac{N_d(\vec{r})}{N_p(\vec{r})} \frac{\int_0^{\infty} N_p(\vec{r}, t) dt}{\int_0^{\infty} N_d(\vec{r}, t) dt} \tag{B71}$$

Since the right side of equation (B71) is a constant, the ratio $N_d(\vec{r})/N_p(\vec{r})$ is a spatially dependent factor which is nonunity if the delayed-neutron fluxes differ from the prompt-neutron fluxes. Let this ratio, the kinetic distortion factor, be defined as $Z^{SO}(\vec{r})$, that is,

$$Z^{SO}(\vec{r}) = \frac{N_d(\vec{r})}{N_p(\vec{r})} \tag{B72}$$

so that equation (B71) becomes for the Sjöstrand method

$$\rho_s(\$) = -\frac{\int_0^\infty N_p(\vec{r}, t)dt}{\int_0^\infty N_d(\vec{r}, t)dt} \cdot Z^{S0}(\vec{r}) \tag{B73}$$

An approximate value for the kinetic distortion factor for the Sjöstrand method may be obtained by using fundamental mode values of $N_d(\vec{r})$ and $N_p(\vec{r})$. That is, let

$$Z_0^{S0}(\vec{r}) = \frac{N_0^S(\vec{r})}{N_0^p(\vec{r})} \tag{B72'}$$

Calculational and Experimental Procedure

Since some of the experimental procedures use calculated parameters, the basic calculations are discussed first. The solution to the various equations can be obtained by using, for example, the S_n method as described in reference 14. The steps in the calculational procedure (C1 to C4) are as follows:

(C1) Solve equation (B24) for the fundamental prompt-mode flux together with equation (B13) for the fundamental static adjoint flux. These two calculations performed together give

(a) Fundamental prompt-mode decay constant, α_0^p

(b) Static multiplication factor, K_{eff}

(c) Total effective fundamental mode delayed-neutron fraction, $\bar{\beta}_0$

(d) Neutron generation time for fundamental prompt mode, Λ_0

(e) Fundamental prompt-mode flux, $\varphi_0^p(\vec{r}, E)$

(f) Fundamental delayed-mode adjoint flux, $\varphi_0^{S+}(\vec{r}, E)$

(g) $F_{00} = \int P_0^{S+}(\vec{r})P_0^p(\vec{r})d\vec{r}$

(C2) Solve equation (B12) for the static flux together with equation (B13) for the static adjoint flux. These two calculations performed together yield

(a) Static multiplication factor, K_{eff}

(b) Fundamental delayed-mode flux, $\varphi_0^S(\vec{r}, E)$

(c) Fundamental delayed-mode adjoint flux, $\varphi_0^{S+}(\vec{r}, E)$

(d) $F_{00}^S = \int P_0^{S+}(\vec{r})P_0^S(\vec{r})d\vec{r}$

(C3) From the calculations described in step (C1), quantities can be obtained which may be compared to experimentally measured values. These are

(a) Fundamental prompt-mode decay constant, which is compared to an experimental determination, α_0^p

(b) Reactivity in dollars computed by the equation (B20a)

$$\rho_s^c(\$) = \frac{K_{eff} - 1}{K_{eff}\bar{\beta}_0}$$

or from the equation (B20b)

$$\rho_s^c(\$) = \frac{\alpha_0^p}{\frac{\bar{\beta}_0}{\Lambda_0}} + 1$$

(C4) Kinetic distortion factors for the various area-ratio methods can be obtained from the computed quantities given in steps (C1) and (C2). The procedure is as follows:

(a) Determine $N_0^s(\vec{r})$ by using equation (B50b):

$$N_0^s(\vec{r}) = \int dE \frac{1}{v(E)} \varphi_0^s(\vec{r}, E)$$

(b) Determine $N_0^p(\vec{r})$ by using equation (B52a):

$$N_0^p(\vec{r}) = \int dE \frac{1}{v(E)} \varphi_0^p(\vec{r}, E)$$

(c) Determine the kinetic distortion factor for the Gozani and Garelis-Russell area-ratio methods based on fundamental mode values, by using equation (B53):

$$Z_0^{G0}(\vec{r}) = \frac{N_0^s(\vec{r})}{N_0^p(\vec{r})} \cdot \frac{F_{00}}{F_{00}^s}$$

$$Z_0^{GR}(\vec{r}) = Z_0^{G0}(\vec{r})$$

(d) Determine the kinetic distortion factor for the Sjöstrand area-ratio method based on fundamental mode values, by using equation (B72'):

$$Z_0^{S0}(\vec{r}) = \frac{N_0^s(\vec{r})}{N_0^p(\vec{r})}$$

The experimental procedure for obtaining reactivities from observed fundamental mode decay constants and measured prompt- and delayed-neutron fluxes is now described. The steps in the experimental procedure (E1 to E6) are as follows:

(E1) Using a repetitively pulsed-neutron source and a $v(E)^{-1}$ neutron detector, obtain the detector response as a function of time. By means of a data processing code (ref. 13), the following information is obtained:

(a) Fundamental prompt-mode decay constant, $\left(\alpha_0^p\right)_E$

(b) Prompt-neutron density for all modes, $N_p(\vec{r}, t)$

(c) Delayed-neutron density for all modes, $N_d(\vec{r}, t)$

(d) Fundamental prompt-mode neutron density, $N_0^p(\vec{r}, t)$

(e) Parameter $Q_0 N_0^p(\vec{r})$ defined by equations (B34), (B52a), and (B31a) and obtained experimentally by fitting the equation

$$N_0^p(\vec{r}, t) = Q_0 \exp\left[\left(\alpha_0^p\right)_E t\right] N_0^p(\vec{r}) \tag{B74}$$

(E2) Compute an "experimental" value of the reactivity in dollars by using $\left(\alpha_0^p\right)_E$ and computed values of $\bar{\beta}_0$ and Λ_0 obtained as in step (C1). Then, the "experimental" value of reactivity based on the inhour method is given by

$$\rho_s^{IN}(\$) = \frac{\left(\alpha_0^p\right)_E}{\frac{\bar{\beta}_0}{\Lambda_0}} + 1 \tag{B75}$$

(E3) Compute the reactivity by using the Gozani extrapolated-area-ratio method. This reactivity is given by evaluating equation (B51), that is,

$$\rho_s^{G0}(\$) = \frac{\int_0^\infty N_0^p(\vec{r}, t)dt}{\int_0^\infty N_d(\vec{r}, t)dt} Z_0^{G0}(\vec{r})$$

$$= \frac{\frac{Q_0 N_0^p(\vec{r})}{\left(\alpha_0^p\right)_E}}{\int_0^\infty N_d(\vec{r}, t)dt} \left[Z_0^{G0}(\vec{r})\right] \tag{B76}$$

Since the delayed-neutron distribution $N_d(\vec{r}, t)$ is assumed to be constant with time, the

integral in the denominator of equation (B76) can be evaluated for a pulse repetition rate R. Then, this gives the reactivity as

$$\rho_s^{G0}(\$) = \frac{\dfrac{Q_0 N_0^p(\vec{r})}{\left(\alpha_0^p\right)_E}}{\dfrac{N_d(\vec{r},t)}{R}} Z_0^{G0}(\vec{r}) \tag{B76'}$$

The kinetic distortion factor $Z_0^{G0}(\vec{r})$ is defined in terms of computed quantities and is given in step (C4).

(E4) Compute the reactivity by using the Garelis-Russell technique. This means finding a value of x such that the following equality is satisfied:

$$\int_0^\infty N_p(\vec{r},t)[\exp(xt) - 1]dt = \int_0^\infty N_d(\vec{r},t)dt \tag{B54}$$

Since the delayed-neutron distribution $N_d(\vec{r},t)$ is assumed to be constant with time, the integral on the right side of equation (B54) can be evaluated for a pulse repetition rate R. This gives

$$\int_0^\infty N_p(\vec{r},t)[\exp(xt) - 1]dt = \frac{N_d(\vec{r},t)}{R} \tag{B54'}$$

Then the reactivity in dollars is given by

$$\rho_s^{GR}(\$) = \left[\frac{\left(\alpha_0^p\right)_E}{x} + 1\right] Z_0^{GR}(\vec{r}) \tag{B77}$$

where $Z_0^{GR}(\vec{r}) = Z_0^{G0}(\vec{r})$.

(E5) Compute the reactivity by using the Sjöstrand area-ratio method (refs. 1 and 12). This reactivity is given as

$$\rho_s^{S0}(\$) = -\frac{\displaystyle\int_0^\infty N_p(\vec{r},t)dt}{\displaystyle\int_0^\infty N_d(\vec{r},t)dt} \cdot Z^{S0}(\vec{r}) \tag{B78}$$

where $Z^{S0}(\vec{r})$ is given by equation (B72). If $N_d(\vec{r},t)$ is constant with time, equation (B78) can be evaluated for a pulse repetition rate R. This gives

$$\rho_s^{S0}(\$) = \frac{-\int_0^{\infty} N_p(\vec{r}, t)dt}{\frac{N_d(\vec{r}, t)}{R}} Z^{S0}(\vec{r}) \qquad \text{(B78')}$$

(E6) Compute the reactivity by using the method of Simmons and King (ref. 5). This reactivity is given by

$$\rho_s^{SK}(\$) = - \frac{\left(\alpha_0^p\right)_E}{\left(\alpha_0^p\right)_E^{DC}} + 1 \qquad \text{(B79)}$$

where $\left(\alpha_0^p\right)_E^{DC}$ is the measured fundamental prompt-mode decay constant of the system at delayed critical.

REFERENCES

1. Sjöstrand, Nils G.: Measurements on a Subcritical Reactor Using a Pulsed Neutron Source. Arkiv Fysik, vol. 11, 1956, pp. 233-246.

2. Gozani, Tsahi: A Modified Procedure for the Evaluation of Pulsed Source Experiments in Subcritical Reactors. Nukleonik, vol. 4, no. 8, 1962, pp. 348-349.

3. Garelis, Edward; and Russell, John L., Jr.: Theory of Pulsed Neutron Source Measurements Nucl. Sci Eng., vol. 16, no. 3, July 1963, pp. 263-270.

4. Preskitt, C. A.; Nephew, E. A.; Brown, J. R.; and Van Howe, K. R.: Interpretation of Pulsed-Source Experiments in the Peach Bottom HTGR. Nucl. Sci. Eng., vol. 29, no. 2, Aug. 1967, pp. 283-295.

5. Simmons, B. E.; and King, J. S.: A Pulsed Neutron Technique for Reactivity Determination. Nucl. Sci. Eng., vol. 3, no. 5, May 1958, pp. 595-608.

6. Corngold, Noel: On the Analysis of Pulsed, Multiplying Systems. Rep. GA-5404, General Dynamics Corp., June 24, 1964.

7. Becker, Martin; and Quisenberry, Karl S.: The Spatial Dependence of Pulsed-Neutron Reactivity Measurements. Symposium on Neutron Dynamics and Control, Univ. Ariz., 1965.

8. Masters, Christopher F.; and Cady, K. B.: A Procedure for Evaluating Modified Pulsed-Neutron-Source Experiments in Subcritical Nuclear Reactors. Nucl. Sci. Eng., vol. 29, no. 2, Aug. 1967, pp. 272-282.

9. Wallace, S. K.; Teare, K. R.; and Green, J. B.: Methods for the Comparison of Pulsed-Neutron Shutdown Measurements with Theory. Nucl. Sci. Eng., vol. 25, no. 4, Aug. 1966, pp. 407-412.

10. Fox, Thomas A.; Mueller, Robert A.; Ford, C. Hubbard; and Alger, Donald L.: Critical Mass Studies with NASA Zero Power Reactor II. I: Clean Homogeneous Configurations. NASA TN D-3097, 1965.

11. Edelmann, M.; Kussmaul, G.; Meister, H.; Stegemann, D.; and Vaeth W.: Pulsed Source and Noise Measurements on the STARK-Reactor at Karlsruhe. Rep. KFK 303, SM62/3, International Atomic Energy Agency Symposium on Pulsed Neutron Research, Karlsruhe, Germany, May 10-14, 1965.

12. Sjöstrand, N. G.: Measurements on a Subcritical Reactor with a Pulsed Neutron Source. Physics of Reactor Design. Vol. 5 of Proceedings of the International Conference on the Peaceful Uses of Atomic Energy. United Nations, 1956, pp. 52-54.

13. Kaufman, N. C.: GRIPE II, A Computer Program for the Analysis of Data from a Pulsed-Neutron Experiment. Rep. IN-1085, Idaho Falls National Reactor Testing Station, Sept. 1967.

14. Fieno, Daniel: Transport Study of the Real and Adjoint Flux for NASA Zero Power Reactor (ZPR-I). NASA TN D-3990, 1967.

15. Joanou, G. D.; and Dudek, J. S.: GAM-II. A B_3 Code for the Calculation of Fast-Neutron Spectra and Associated Multigroup Constants. Rep. GA-4265, General Dynamics Corp., Sept. 16, 1963.

16. Joanou, G. D.; Smith, C. V.; and Vieweg, H. A.: GATHER-II. An IBM-7090 Fortran-II Program for the Computation of Thermal-Neutron Spectra and Associated Multigroup Cross Sections. Rep. GA-4132, General Dynamics Corp., July 8, 1963.

17. Keepin, G. Robert: Physics of Nuclear Kinetics. Addison-Wesley Publ. Co., 1965.

18. Alger, Donald; Mayo, Wendell; and Mueller, Robert: Measurement of Effective Delayed Neutron Fraction for NASA Zero Power Reactor I. NASA TN D-3709, 1966.

19. Gross, E. E.; and Marable, J. H.: Static and Dynamic Multiplication Factors and Their Relation to the Inhour Equation. Nucl. Sci. Eng., vol. 7, no. 4, Apr. 1960, pp. 281-291.

20. Garelis, Edward: Theory of Pulsing Techniques. Nucl. Sci. Eng., vol. 18, no. 2, Feb. 1964, pp. 242-245.

NASA-Langley, 1969 — 22 E-5086

"The aeronautical and space activities of the United States shall be conducted so as to contribute . . . to the expansion of human knowledge of phenomena in the atmosphere and space. The Administration shall provide for the widest practicable and appropriate dissemination of information concerning its activities and the results thereof."

—NATIONAL AERONAUTICS AND SPACE ACT OF 1958

NASA SCIENTIFIC AND TECHNICAL PUBLICATIONS

TECHNICAL REPORTS: Scientific and technical information considered important, complete, and a lasting contribution to existing knowledge.

TECHNICAL NOTES: Information less broad in scope but nevertheless of importance as a contribution to existing knowledge.

TECHNICAL MEMORANDUMS: Information receiving limited distribution because of preliminary data, security classification, or other reasons.

CONTRACTOR REPORTS: Scientific and technical information generated under a NASA contract or grant and considered an important contribution to existing knowledge.

TECHNICAL TRANSLATIONS: Information published in a foreign language considered to merit NASA distribution in English.

SPECIAL PUBLICATIONS: Information derived from or of value to NASA activities. Publications include conference proceedings, monographs, data compilations, handbooks, sourcebooks, and special bibliographies.

TECHNOLOGY UTILIZATION PUBLICATIONS: Information on technology used by NASA that may be of particular interest in commercial and other non-aerospace applications. Publications include Tech Briefs, Technology Utilization Reports and Notes, and Technology Surveys.

Details on the availability of these publications may be obtained from:

SCIENTIFIC AND TECHNICAL INFORMATION DIVISION

NATIONAL AERONAUTICS AND SPACE ADMINISTRATION

Washington, D.C. 20546